Journal Pre-proof

Iron slag/activated carbon-electrokinetic system with anolyte recycling for single and mixture heavy metals remediation

Faris M. Hamdi, Ali Altaee, Lilyan Alsaka, Ibrar Ibrar, Maryam AL-Ejji, John Zhou, Akshaya K. Samal, Alaa H. Hawari

PII:	S0048-9697(24)02662-7
DOI:	https://doi.org/10.1016/j.scitotenv.2024.172516
Reference:	STOTEN 172516
To appear in:	*Science of the Total Environment*
Received date:	10 October 2023
Revised date:	2 April 2024
Accepted date:	14 April 2024

Please cite this article as: F.M. Hamdi, A. Altaee, L. Alsaka, et al., Iron slag/activated carbon-electrokinetic system with anolyte recycling for single and mixture heavy metals remediation, *Science of the Total Environment* (2024), https://doi.org/10.1016/j.scitotenv.2024.172516

Iron slag/activated carbon-electrokinetic system with anolyte recycling for single and mixture heavy metals remediation

Faris M. Hamdi[1,2], Ali Altaee[1*], Lilyan Alsaka[1], Ibrar Ibrar[1], Maryam AL-Ejji[3], John Zhou[1], Akshaya K. Samal[4], Alaa H. Hawari[5]

1. Centre for Green Technology, School of Civil and Environmental Engineering, University of Technology Sydney, 15 Broadway, NSW 2007, Australia
2. Department of Civil Engineering, Jazan University, Jazan 82822, Saudi Arabia
3. Center of Advanced Materials, Qatar University, PO Box 2713, Doha, Qatar
4. Centre for Nano and Material Sciences, Jain University, Ramanagara, Bangalore 562 112, Karnataka, India
5. Department of Civil and Environmental Engineering, College of Engineering, Qatar University, PO Box 2713, Doha, Qatar

** Corresponding author; E-mail address: ali.altaee@uts.edu.au*

Graphical Abstract

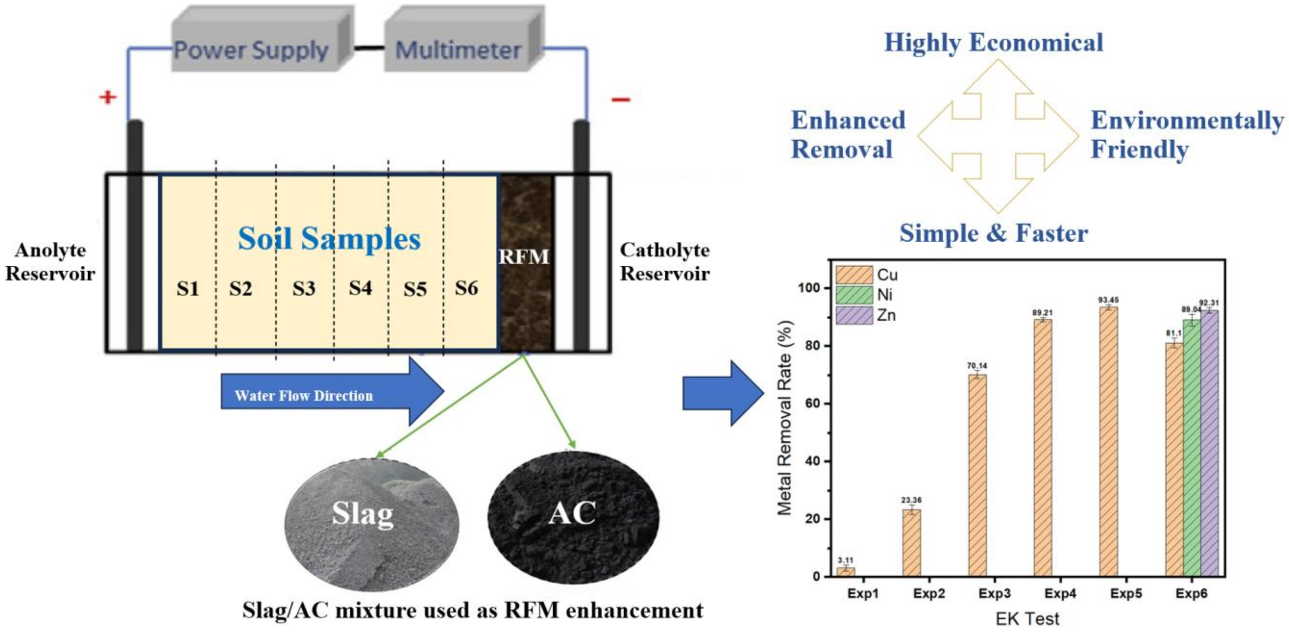

Abstract:

The electrokinetic process has been proposed for in-situ soil remediation to minimize excavation work and exposure to hazardous materials. The precipitation of heavy metals in alkaline pH near the cathode is still challenging. Reactive filter media and enhancement agents have been used in electrokinetics to enhance the removal of heavy metals. This study investigated coupling industrial iron slag waste and iron slag-activated carbon reactive filter media with electrokinetic for a single and mixture of heavy metals treatment. Instead of using acid enhancement agents, the anolyte solution was recycled to neutralize the alkaline front at the cathode, reducing the operation cost and chemical use. Experiments were conducted for 2 and 3 weeks at 20 mA electric current. Copper removal increased from 3.11% to 23% when iron slag reactive filter media was coupled with electrokinetic. Copper removal increased to 70.14% in the electrokinetic experiment with iron slag-activated carbon reactive filter media. The copper removal increased to 89.21% when the anolyte solution was recycled to the cathode compartment. Copper removal reached 93.45% when the reactive filter media-electrokinetic process with anolyte recirculation was extended to 3 weeks. The reactive filter media- an electrokinetic process with anolyte recycling was evaluated for removing copper, nickel, and zinc mixture, and results revealed 81.1% copper removal, 89.04% nickel removal, and 92.31% zinc removal in a 3-week experiment. The greater nickel and zinc removal is attributed to their higher solubility than copper. The results demonstrated the cost-effectiveness and efficiency of the electrokinetic with iron slag-activated carbon reactive filter media with anolyte recirculation for soil remediation from heavy metals.

Keywords: Electrokinetic, Anolyte recirculation, Soil remediation, Iron slag, Reactive filter media

1. Introduction

The presence of heavy metal contaminants in soils has become a matter of global significance, primarily because of their toxic nature, long-lasting effects, and the potential risk they pose to food safety (Wen et al., 2021). Numerous strategies and techniques have been proposed to address soil contamination problems (Song et al., 2017). In addition to traditional decontamination methods, electrokinetic has been suggested for low permeability soil treatment at a low cost (Agnew et al., 2011) by placing electrodes strategically in polluted soil to induce heavy metal transport under the effect the electric field across the soil (Peppicelli et al., 2018). The precipitation of heavy metals near the cathode adversely affects the EK process, increasing the soil resistivity to electric current and complicating contaminants extraction (Yeung, 2011). As a result, there is an increasing demand to improve the EK method to stop the advancement of the alkaline front and maintain the soil pH low enough for heavy metals removal (Yuan et al., 2016b; Ghobadi et al., 2021a; Wen et al., 2021).

Researchers have focused on improving the EK process and making it more practical by incorporating enhancement agents like chelating and surfactants to boost contaminant mobility. Acidic or basic solutions were also used to regulate the pH of the electrolyte (Ganbat et al., 2022; Ghobadi et al., 2021b; Li et al., 2020). While there has been a considerable amount of research on the electrokinetic (EK) process in soil remediation, only a limited number of studies have focused explicitly on remediating soil contaminated with a mixture of heavy metals (Bahemmat et al., 2016; Yuan et al., 2016b). Yuan et al. (2016a) investigated the use of an assisting agent, citric acid combined with calcium chloride (CA+$CaCl_2$), for the simultaneous removal of five heavy metals (namely Zn, Cd, Ni, Cu, and Pb) from contaminated kaolin. This example closely resembles real-world scenarios where polluted soil is frequently affected by a mixture of various heavy metals rather than being polluted by a single metal ion alone. The study reported varying removal efficiencies ranging from 86.2% to 99.0% for Zn, Ni, Cd, Cu, and Pb. Also, in a study conducted by (Yuan et al., 2016a), the researchers investigated the impact of carbon nanotube-covered polyethylene terephthalate yarns (PET-CNT) when used as a cathode electrode in the simultaneous electrokinetic remediation of multi-heavy metals (Zn, Ni, Cd, Cu, and Pb) contaminated kaolin. Introducing PET-CNT as the cathode electrode significantly increased the electric current and electroosmotic flow while reducing the soil pH, leading to enhanced extraction efficiencies of the heavy metals. The study's findings revealed that the order of heavy metal removal efficiency decreased in the following sequence: Ni > Cd > Zn > Cu > Pb, indicating that Ni, Cd, and Zn were relatively easier to extract from the contaminated soil compared to Cu and Pb, which posed greater challenges for removal. However, selecting the proper enhancement technique is essential in the EK process concerning treatment duration, cost, and environmental impact. For instance, it is possible to affect the soil matrix when applying the enhancement agent. Consequently, it becomes necessary to recover the electrolyte after the EK treatment (Ghobadi et al., 2020; Lim et al., 2016). Indeed, despite the widespread use of enhancing agents in the EK process, laboratory-scale studies have revealed the adverse effects of strong acids on specific soil characteristics, such as electrical conductivity and pH, post-treatment. Moreover, applying these agents increased remediation costs due to the need for electrolyte recovery after the EK treatment (Gong et al., 2018; Mao et al., 2015). Certain enhancement agents are not recommended for extracting heavy metals because of their unsuccessful applications in full-scale EK operations (Bahemmat et al., 2016; Gong et al., 2018). Tian et al. (2017) explored the use of eco-friendly enhancing agents like rhamnolipids, saponin, and citric acid in the EK remediation process to address soil contamination with Cd, Cr, Cu, Pb, Zn, and PAH/PCB in harbour sediments. Results revealed that the combination of these agents only managed to remove small amounts of metals (4.4% to 15.8%) and achieved a slightly better removal rate for PAH (29.2%) and PCB (38.2%) (Tian et al., 2017).

Bio-EK remediation, considered one of the most environmentally friendly options for extracting heavy metals from the soil, may require a longer remediation time, albeit relatively inexpensive (Gong et al., 2018). The simultaneous extraction of heavy metals has also been investigated by implementing EK remediation coupled with reactive filter media (RFM), another technique to enhance metal ion removal by the EK process. Researchers suggested several types of RFMs for soil remediation by the EK process, including activated carbon (AC), zerovalent iron (ZVI), and charcoal made from the activation of bamboo (Cang et al., 2009a; Gholizadeh and Hu, 2021; Ren et al., 2014; Yuan and Chiang, 2007; Zhao et al., 2016). The factors that should be considered in selecting the RFM media are cost, efficiency, availability, ease of use and recycling, and lifetime of the RFM (Ghobadi et al., 2021b, 2020). Ghobadi et al. (2021b) investigated the utilization of a compost or biochar mixture as a reactive filter material (RFM) combined with an electrokinetic remediation (EKR) process to treat copper-polluted kaolin. According to their laboratory findings, the EK-RFM process, with the application of a constant electric current and the use of EK with 100% compost treatment, significantly enhanced the removal of copper from 1.03% to an impressive 84.09%. However, it's worth noting that this improvement in removal efficiency was accompanied by increased energy consumption. Contrarily, adding different grades of biochar to the compost in the soil during the EK-RFM process did not improve the removal of Cu ions. In addition, the overall Cu removal dropped from 84.09% to 74.11% when the compost was renewed and reused during the EK process. The study's results highlight compost as a promising and environmentally friendly reactive filter material (RFM) that enhances heavy metal removal in the EK process, especially when a continuous electric current is applied to lower the soil's pH due to its diverse organic compounds. In a consecutive study, Ghobadi et al. (2021a) investigated the removal of a mixture of heavy metals from natural soil using compost as an RFM. The study achieved a significant removal of Zn, Cd, and Mn, ranging from 51.6% to

72.1%, while Pb and Cu, resulting in smaller extractions of 28.2% and 29.1%, in conjunction with an electric current of 30.00 mA for a treatment duration of 14 days. The presence of soil organic matter had an adverse effect on the mobilization and migration of heavy metals, including Cu and Pb.

In 2021, Xie et al. conducted a study that combined the EK process with AC and Citric Acid (CA) to treat natural lead-contaminated soil by mixing the lead-contaminated soil with $Pb(NO_3)2$ solution to create the lead-contaminated soil. A concern arose during one test using only CA with the EK technique, as a high pH of approximately 13 was observed near the cathode. This high pH led to the accumulation of metal ions adjacent to the cathode, clogging the soil pores and significantly hindering the treatment process. However, a remarkable improvement was observed when RFM added AC to the EK process with CA. The lead removal efficiency increased dramatically from 15% to 58% within 20 days. Because of its excellent efficacy in removing various heavy metal contaminants, AC is extensively employed in soil and water treatment as an adsorbent. Due to its extensive surface area, AC efficiently eliminates metal pollutants from the soil through surface adsorption. Despite its advantages, insufficient quantities of acceptable AC and the high production cost pose disadvantages to using AC RFM (Ahmed et al., 2015; Alhashimi and Aktas, 2017; Xie et al., 2021).

Yu et al. (2019) explored the application of EK combined with RFM to treat Cr(VI)-contaminated soil. Two types of RFM were employed: CTMAB-Z, a modified zeolite prepared with cetyltrimethyl ammonium bromide, acting as RFM-1, and a combination of CTMAB-Z and Fe(0) serving as RFM-2. Additionally, the study investigated the impact of chemical enhancers/additives, specifically DL-tartaric acid and Tween 80, on the EK of Cr(VI) in a series of contrasting experiments. Furthermore, the multifactor orthogonal investigation revealed that the highest Cr(VI) removal rate (80.92%) and leaching efficiency (85.25%) were obtained when the samples were treated with a voltage gradient of 2.5 V cm^{-1} for eight days. The study effectively demonstrated that the EKR process for Cr(VI) remediation could be significantly enhanced by incorporating RFM and additives. Another RFM commonly used due to its high adsorption and low cost is zerovalent iron (ZVI) (Cang et al., 2009b; Ren et al., 2014; Yu et al., 2019; Zhao et al., 2016). According to Cang et al. (2009a), combining EK remediation with a ZVI RFM resulted in 72% Cr removal from the soil. However, the precipitation of contaminants on the ZVI surface controls its lifespan. Moreover, exposure to silica or natural organic materials can decrease the reactivity of the ZVI (Cang et al., 2009a; Ren et al., 2014). To address the limitations of using chemical agents in the EK process, researchers constructed RFM with activated carbon (AC), activated bamboo charcoal, and zerovalent iron (Ren et al., 2014; Xue et al., 2017). Despite their benefits, the widespread application of these RFMs is hindered by cost, availability, and life cycle concerns. Additionally, RFMs alone may not be sufficient to halt the advancement of the alkaline front, necessitating the use of additional chemical reagents, thereby reducing the overall cost-effectiveness of the EK treatment (Cang et al., 2009b; Ren et al., 2014; Zhao et al., 2016).

This study investigated coupling the EK process with industrial iron slag waste and iron slag/AC RFM for a single or mixture of contaminants removal from kaolinite soil. Iron slag was selected because it is an industrial waste with excellent adsorption to metal ions and is available. The kaolinite soil spiked with Cu, Ni, and Zn ions are common contaminants and were tested for EK decontamination as a standalone or mixture of contaminants. The iron slag alkalinity pH 11 is suitable for metal ions precipitation when captured by the RFM. The study also implemented a new technique of anolyte recycling to neutralize alkaline pH at the cathode and promote acid front transport across the soil. The method replaces using chemical agents for alkaline front neutralization to reduce chemical use. The research questions are: i) what is the efficiency of metal ions removal from kaolinite with and without iron slag RFM, ii) what is the effect of anolyte recycling to the cathode zone on metal ions removal during the EK process, and iii) what is the effect of multiple contaminants in the kaolinite soil on the efficiency of the electrokinetic remediation process? The study also investigated the impact of the RFM, EK duration, iron slag to AC ratio, and metal ion types on the EK remediation efficiency.

2. Materials and methods

2.1. Sample Preparation and Analytical Methods

All chemicals were in a laboratory and used without modifications. Copper sulphate, zinc sulphate, and nickel chloride, 99% purity, were acquired from Sigma Aldrich (Australia). Kaolin soil was acquired from Keane Ceramic Pty (Australia) and investigated in the EK tests because of its purity and low organic and inorganic contaminants. The local steel manufacturing industry (Australia) provided the iron slag (InfraBuild, Rooty Hill NSW 2766). The RFM was either iron slag alone or a mixture of iron slag and AC (Sigma-Aldrich, Australia). The soil's and RFM's chemical and physical characteristics are listed in **Tables 1** and **2**, respectively.

One liter of distilled water was mixed with 1000 grams of kaolin soil, and the mixture was stirred for 30 minutes with 2.52 grams of CuSO4, 2.21 grams of NiCl2, and 2.51 grams of $ZnSO_4$. Before loading into the EK cell (**Figure 1**), the prepared soil is stored for at least 72 hours while constantly stirring to ensure the heavy metals adsorption onto the soil reaches equilibrium (Altaee et al., 2008). During loading, a manual compactor was used to consolidate the contaminated soil in layers to guarantee that no voids were formed. The morphological and chemical characteristics of the RFMs (Reactive Filter Media) were assessed through Energy Dispersive X-ray (EDX). Fourier Transform Infrared Spectroscopy (FTIR) using the Miracle-10 instrument (Shimadzu) was employed to analyze the surface functional groups of the RFMs before and after the EK tests. To determine the RFM's specific surface area, the Brunauer-Emmett-Teller (BET) nitrogen adsorption-desorption isotherms tests were conducted pre- and post-EK treatment. The Barrett-Joyner-Halenda (BJH) method was also utilized for a post-EK treatment analysis. These measurements were performed using a Micrometrics 3-FlexTM surface characterization analyzer at 77K.

Table 1: Property of kaolinite clay soil

Soil characteristics	Range of values
Particles size analysis	
Clay	45.80
Silt	50.16
Sand	2.12
Permeability (m/sec)	3.95×10^{-10}
Density (g/cm^3)	1.35
Porosity (kg/m^3)	599
Organic matter	NIL
TDS (ppm)	129
pH	4.24 ± 0.04
Electrical conductivity (mS/cm)	0.39 ± 0.010
Initial copper concentration (mg /kg)	990

Table 2: Different physicochemical characteristics of RFM

Parameter	Iron slag	Iron slag/AC (50/50)
Particle size analysis (%)		
Greater than 2 mm	2.61	2.48
In between 1-2 mm	-	-
Less than 1mm	-	-
Permeability of soil ($m\ s^{-1}$)	1.67×10^{-3}	2.54×10^{-2}
Specific Surface area (m^2g^{-1})	0.037	146.57
pH	11.38	10.63
Electrical conductivity (mS/cm)	0.643	0.551

2.2. Electrokinetic cell setup

Figure 1 displays a schematic diagram of the EK experimental apparatus and the EK cell employed in this study. The EK experiments were carried out in a reactor measuring 23 cm x 8 cm x 11 cm constructed with plexiglass material to enable easy optical monitoring. At either end of the sample compartments are two electrode compartments, and the reactor also consists of contaminated soil in a compartment. Two graphite rod electrodes (15 cm x 1 cm) were purchased from Graphite Australia Pty Ltd and applied the electric current by connecting with a power supply (EAPS-3015-11B) from both ends. A current meter measures the current every hour (Keithley 175 Autoranging multimeter). Two different types of cellulose filter sheets (pore size in the range of 5-13 µm, LLG Labware) were placed between the electrode compartments and the soil to prevent the infiltrating of soil particles into the electrolyte cells while being supported by a perforated plexiglass plate. The RFM was placed in the soil near the cathode compartment. Milli-Q water was intermittently added to the anolyte compartment to compensate for water losses brought on by water electrolysis and electroosmotic flow.

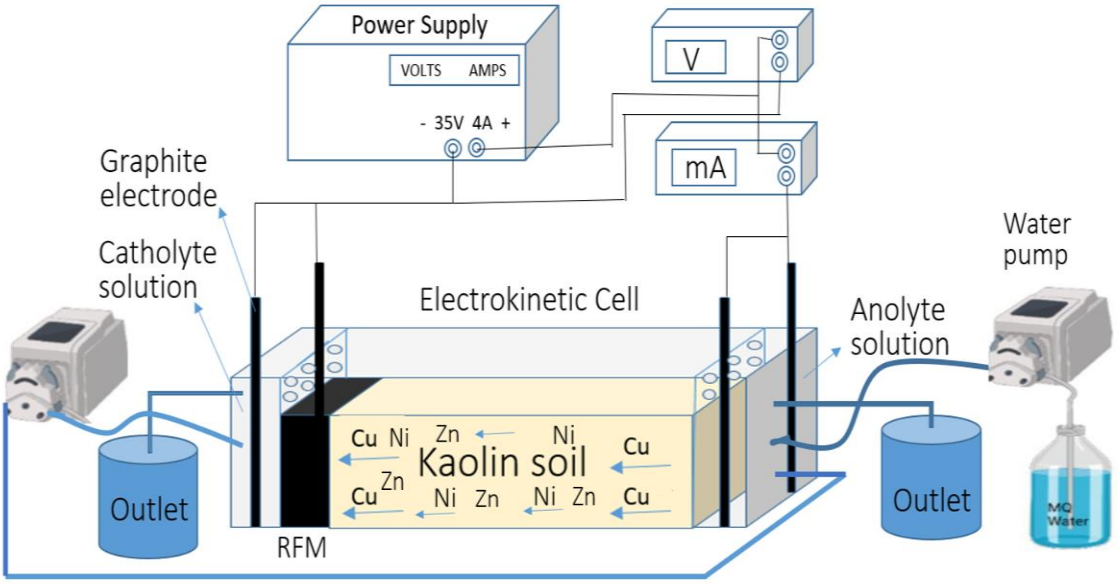

Figure 1: Schematic Cu, Ni, and Zn removal diagram in the EK-RFM reactor.

2.3. Test design

Six electrokinetic experiments were conducted to evaluate the removal of single and mixed heavy metals from the contaminated soil. The first five experiments investigated the removal of copper with and without iron slag/AC RFM, while the sixth experiment aimed at removing mixtures of copper, nickel, and zinc contaminants, as described in **Table 3**. The electrodes were subjected to a constant 20mA current in all tests. The experiments were terminated after 14 days, except for Exp5 and 6, which terminated after 21 to study the impact of the EK duration on heavy metals removal. The experiments were conducted at 1000 mg/kg Cu, Ni, and Zn concentration, RFM weight of 100 g near the cathode area, and 20 mA electric current.

Exp1 was a typical EK experiment with kaolinite, for which 1000 mg/kg Cu was added. Exp2 and 3 were performed to study the effect of the slag or slag/AC RFM on removing Cu from kaolinite soils by the EJ process. Exp4 and Exp5 were conducted to study the effect of slag/AC RFM with anolyte recycling on Cu removal from the kaolin soils in 14 days in Exp4 and 21 days in Exp5. Low-pH anolyte recycling to the cathode is used to control the alkaline front movement in the soil. Finally, with an anolyte recycling test, the Exp6 slag/AC RFM-EK system was performed for 21 days to evaluate the efficiency of removing Cu, Ni, and Zn from the kaolin.

Once the experiments were completed, the aqueous solutions were collected from the anode, cathode, and electrode assemblies. The kaolin soil was divided into six equal sections and kept separately in the designated plastic bag. Then, each section was homogenized before taking samples for metal ion measurement. Each soil sample's pH, conductivity, and Cu, Ni, and Zn concentrations were measured in triplicates.

Table 3. The type of EK tests and heavy metals concentration is 1000 mg/kg

No of Exp	Experiment type	Heavy metal	Metal concent. (mg/kg)	Anolyte recycling	RFM	Current (mA)	Time (day)

Exp1	EK only	Cu	1000	NA	NA	20	14
Exp2	EK-Iron slag	Cu	1000	NA	100% Iron slag	20	14
Exp3	EK- Iron slag /AC	Cu	1000	NA	50% Iron slag+50%AC	20	14
Exp4	EK- Iron slag /AC	Cu	1000	Anolyte	50% Iron slag+50%AC	20	14
Exp5	EK- Iron slag /AC	Cu	1000	Anolyte	50% Iron slag+50%AC	20	21
Exp6	EK- Iron slag /AC	Cu, Ni, Zn	1000	Anolyte	50% Iron slag+50%AC	20	21

2.4. RFM adsorption/desorption tests

The adsorption capacity of the iron slag/AC was assessed employing a thermostatic shaker under controlled conditions at a consistent ambient temperature of 25 ± 1°C, with a rotational velocity of 150 revolutions per minute (rpm) sustained for a duration spanning from 3.5 to 24 hours. The solid-to-liquid ratios for copper sulfate and the mixed solution were 2.52 g/L, while the mixed solution was 2.52 g/L for copper sulfate, 2.21 g/L for nickel chloride, and 2.51 g/L for zinc sulfate, respectively. The adsorbents (a combination of iron slag and AC in a 1:1 ratio) were employed to assess their capacity for adsorbing heavy metals. After the adsorption process, the iron slag/AC was isolated using centrifugation at 10000 rpm for 15 minutes. Copper, nickel, and zinc concentrations within the samples were evaluated via Inductively coupled Plasma mass spectroscopy (ICP-MS) analysis. The adsorption capacity (measured in mg/g) was estimated using Equation (1).

$$\text{Adsorption capacity } q_e\left(\frac{mg}{g}\right)=\frac{(C_{initial}-C_{residual})*V}{W} \quad (1)$$

The adsorption capacity equation includes $C_{initial}$: initial Cu, Ni, Zn concentration (in mg/L), $C_{residual}$: equilibrium Cu, Ni, Zn concentration (in mg/L), V: solution volume (in L), and W: iron slag/AC weight (in g). Heavy metal adsorption onto the iron slag/AC is assessed by creating breakthrough curves using the C_f/C_i ratio. Here, C_i signifies the initial pollutant concentration, while C_f represents the contaminant concentration at a particular time, *t*. Breakthrough curve experiments identify the breakthrough point, indicating when the effluent concentration reaches a set percentage of the influent concentration (Rahchamani et al., 2011).

Immediately after the adsorption test, desorption experiments were conducted to assess reversibility and quantify the release of adsorbed heavy metals. A 0.1 M hydrochloric acid (HCl) solution (50 mL) was added to the iron slag/AC mixture in vials. The desorption process occurred on a thermostatic shaker at 25°C and 150 rpm for 24 hours. Subsequently, the iron slag/AC was separated from the solution via centrifugation at 10000 rpm for 15 minutes. Copper, nickel, and zinc concentrations in the samples were determined using inductively coupled plasma (ICP) analysis. Desorption capacity (mg/g) was calculated using Equation (2).

$$Desorption\left(\frac{mg}{g}\right) = \frac{(C_{residual})*V}{W} \tag{2}$$

$C_{residual}$ represents the equilibrium residual concentration of Cu, Ni, and Zn (mg/L), V is the solution volume in litres (L), and W stands for the weight of iron slag/AC in grams (g).

The economic advantages of reusing adsorbents across multiple cycles are evident in reducing adsorption process costs. This attribute is particularly valuable for extensive industrial applications. Adsorption-desorption experiments were conducted in a single cycle to assess the reusability of the adsorbents. The desorption tests were conducted in an acidic environment with a pH of 1.4. The desorption (D) was calculated using Equation (3).

$$D\,(\%) = \left(\frac{C_{desorbed}}{C_{adsorbed}}\right) * 100 \tag{3}$$

In Equation (3), $C_{desorbed}$ represents the desorbed metal ions, and $C_{adsorbed}$ shows the adsorbed metal ions.

2.5. Analytical methods

At the end of the EK experiments, the soil was divided into six equal sections, i.e., S1 to S6. Each section of soil was homogenized and dried in an oven at 105 °C for 12 hours. The soil samples were then prepared to measure pH, conductivity, and Cu concentration for Exp1 to Exp5 and nickel and zinc for Exp6. A soil suspension was made with 1:5 (w/v) dry soil to distilled water and stirred on a magnetic mixer for at least five minutes before using a multimeter (model HACH HQ40d) to measure the kaolinite soil's pH and electric conductivity (EC). The ICP-MS was used to analyze the concentrations of copper, nickel, and zinc. Two samples were extracted from each section after the soil sections were dried and homogenized.

Each sample underwent digestion using 2M nitric acid, with 10 ml of nitric acid added to 1 gram of dry soil (Groenenberg et al., 2017). The soil-acid mixture was then agitated using a shaker for 4 hours, and the soil suspension was centrifuged at 3,000 rpm for three minutes to separate the solution from the soil particles. The RFM was extracted similarly to soil samples and analyzed for Cu, Ni, and Zn concentrations. Heavy metal removal efficiency, as well as the consumption of specific energy (SEC) during the electrokinetic system of (EK) operations, were determined using equations (4) and (5) as described in the studies by Ghobadi et al. (2021 and 2020) respectively. These equations were used to quantify heavy metal removal efficiency and the EK process's energy efficiency.

$$\text{Removal efficiency} = \frac{C_i - C_f}{C_i} 100\ \% \tag{4}$$

$$\mathrm{E_u} = \frac{10^{-3}}{\mathrm{V_s}} \int_0^t VIdt \tag{5}$$

where C_i: initial concentration of the heavy metal (in mg/kg), C_f: residual concentration of the heavy metal (in mg/kg) after the EK experiment; E_u: specific power consumption (in kWh/kg), I: electric current (in A), V: applied voltage (in V), t: experimental time (in hours), and Vs: the total amount of soil treated (in kg).

3. Results and discussion

3.1. Electric current

Contaminant transport across the soil during the electrokinetic treatment is significantly influenced by the applied electrical current, which strongly correlates with free ion concentration (Ghobadi et al., 2020). Therefore, the electrical current is a crucial factor that directly impacts the effectiveness of contaminants' movement in the soil (Ghobadi et al., 2021a). Initially, the electric current in the EK experiment was kept at 20 mA. **Figure 2a** illustrates the variation of electric current during the ED experiments Exp1 to (Ghobadi et al., 2021b, 2021a)Exp6. Water electrolysis produces H^+ and OH^- ions at the anode and cathode, respectively, and the electric current increases due to the ions' migration towards the electrode of an opposite charge (Ganbat et al., 2022). Metal ions dissolution occurs due to the advancement of acid front towards the cathode, increasing the ionic strength of pore fluid. Still, the influx of ionic species decreases over time due to the neutralization of acid and base front when they meet in the soil and the precipitation of metal ions (Ghobadi et al., 2020).

The EK electric current decreases over time due to the metal ions precipitating near the cathode region at alkaline soil pH (Ganbat et al., 2022). The dropdown in the electric current could be due to metal hydroxide precipitation, fouling of the electrodes, or acid and hydroxide fronts meeting near the cathode. After 72 to 96 hours, a decline was observed in the electric current of Exp1 to Exp6. The sharpest drop in electric current was in Exp1, conducted without RFM or anolyte recycling to the cathode, allowing the advancement of the alkaline front in the soil. A similar observation was recorded in Exp2, conducted with 100% iron slag RFM, in which the electric current decreased from 20 mA to 17 mA after 72 h and reached 3 mA after 240 h before it jumped to 4.5 mA after 264 h and reached 5.6 mA at the end of the experiment. The erratic change in the Exp2 electric current could be due to the solubilization of ionic species caused by acid front movement at a later stage of the EK test. Experiment Exp3 was conducted using 50% iron slag mixed with 50% activated carbon (AC) to buffer alkaline front advancement in the soil. The maximum electric current in experiment Exp3, 19 mA, was slightly lower than in experiment Exp2 because of the lower electric conductivity of the RFM in experiment Exp3 (**Table 2**). There was a sharp drop in the electric current from 19 mA to 12.5 mA after 120 h due to metal hydroxide precipitation and acid and alkaline front meeting in the soil. At the end of experiment Exp3, the electric current reached 10 mA, which is 78% greater than the current in experiment Exp2. Incorporating AC in the RFM of experiment Exp3 probably slowed down the advancement of the alkaline front, hence meeting with the acid front, resulting in a higher electric in experiment Exp3.

Experiment Exp4 operating conditions were similar to experiment Exp3, with the anolyte being recycled to the cathode well to neutralize the alkaline front, allowing the acid front to sweep across the soil. The electric current of experiment Exp4 was 20 mA for about 24 h, declined to 14.2 mA after 72 h, and progressively decreased to 6 mA at the end of a 2-week test. When the EK duration increased to three weeks in experiment Exp5, the electric current was 20 mA for 48 h, slightly decreased to 16.3 mA after 72 h, and gradually decreased to 5.5 mA after 504 h. The decrease in experiment Exp5 electric current indicates a steady state operating condition where alkaline front neutralization by the anolyte circulation facilitated the steady advancement of the acid front in the soil and solubilization and precipitation of metal ions near the cathode. Experiment Exp6 was conducted for 3 weeks with multiple heavy metal pollutants, i.e., Cu^{2+}, Ni^{2+}, and Zn^{2+}, to evaluate the EK efficiency for treating soil contaminated with a heavy metals mixture. The electric current of 19.5 mA lasted for 96 h due to the higher ionic strength in experiment Exp6 than in experiment Exp5. After 120 h, the electric current in experiment Exp6 dropped to 15.2 mA, gradually decreasing, and reached 3.8 mA at the end of the 3-week experiment. The lower recorded electric current at the end of experiment Exp6 compared to experiment Exp5 was attributed to the precipitation of metal ions as they approached the cathode compartment. The precipitation of Cu^{2+}, Ni^{2+}, and Zn^{2+} at different pHs increased the soil resistivity, causing a further decline in the electric current of experiment Exp6 compared to experiment Exp5.

As depicted in **Figure 2b,** a negative correlation exists between the electric current and the alteration in voltage. Metal ions precipitation diminished the electric current, increasing the voltage due to the increased soil resistivity. In all EK experiments, the voltage decreased during the first 24 h due to the solubilization of metal ions and increased ionic strength of pore fluid.

The initial voltage was between 18 and 28 V, then decreased to about 11 V after 24 hours. The voltage increased to about 35 V in experiments Exp1, Exp2, Exp4, and Exp5 after 72 h and in experiments Exp3 and Exp6 after 120 h due to the high soil conductivity and ionic strength in experiments Exp3 and Exp6. Compared to a conventional EK process, EK experiments incorporated the RFM with or without anolyte recycling, which exhibited a higher electric current.

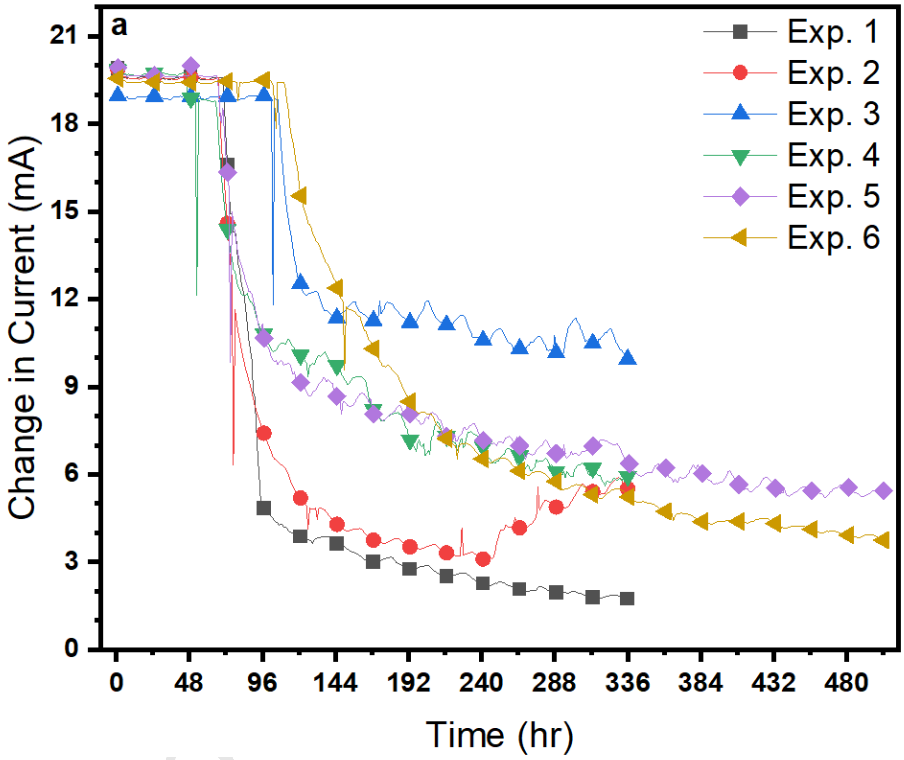

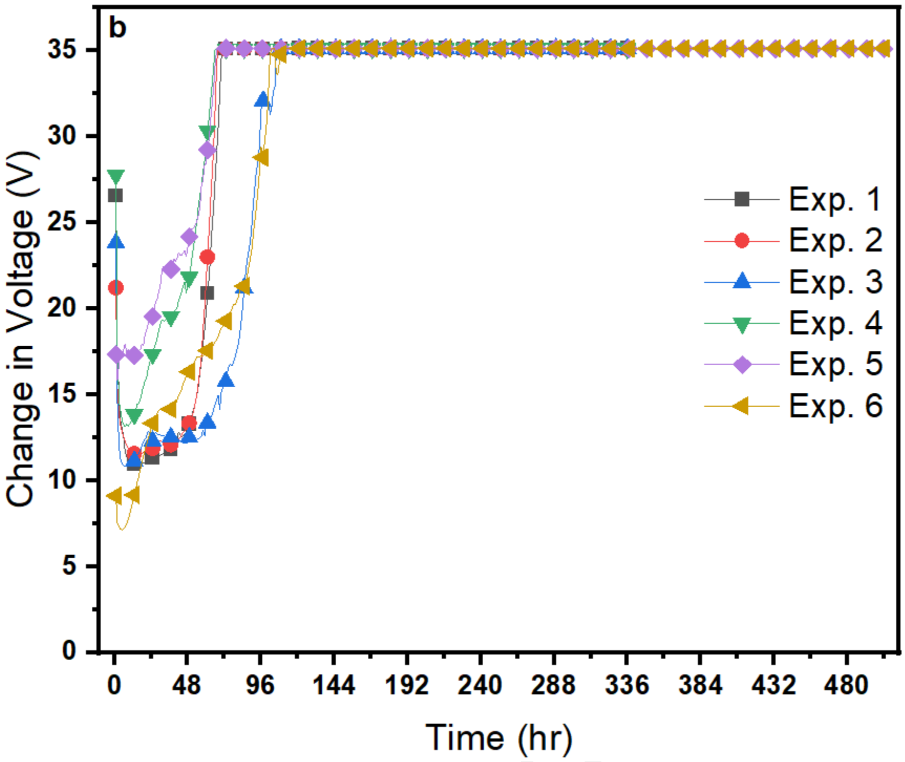

Figure 2: (a) Change in Current (mA) in the electrokinetic experiments and (b) Change in Voltage (V). Experiments were conducted at 20 mA direct current.

3.2. Soil pH and Electric conductivity

Figure 3a shows the pH of soil sections S1 to S6 and the RFM for the EK experiments Exp1 to Exp6. The main electrode reactions at the cathode and anode generate OH^- and H^+ ions according to the reactions below:

$$2H_2O - 4e^- \Rightarrow O_2 + 4H^+ \text{ (anode)} \tag{6}$$

$$4H_2O + 4e^- \Rightarrow 2H_2 + 4OH^- \text{ (cathode)} \tag{7}$$

According to Equation (6), the electrolytic reaction at the anode generates H^+, which migrates towards the cathode, reducing the soil pH. The alkaline soil pH at the cathode is due to the generation and migration of OH^- towards the anode region (Equation 7). The H^+ ions' effective ionic mobility is about 1.8 times larger than the OH^- ions, signifying that H^+ ions exhibit greater mobility and displacement in the soil than the OH^- ions (Acar and Alshawabkeh, 1993).

The initial soil pH was about pH 4.24 (**Table 1**). The soil pH decreased to less than the initial soil pH for sections S1 to S5 and was higher than in section S6 for experiments Exp1 to Exp3, whereas it was close to or slightly lower than soil pH in section S6 for experiments Exp4 to Exp6 (**Figure 3a**). For experiments Exp1 to Exp3, the soil pH was about pH 3 in section S1, increased slightly in the soil sections S2 and S3, and reached pH 4 in section S4. The soil pH of section S6 jumped to about 6.5 in experiment Exp1, pH 7 in experiment Exp2, and pH 5.2 in experiment Exp3. Compared to experiment Exp1, the higher soil pH in section S6 of experiment Exp2 was attributed to the 100% iron slag RFM (pH 11.38), which promoted alkaline front movement in the soil. However, mixing 50% AC in the iron slag RFM buffered alkaline pH movement towards the anode, and hence, the acid front advanced towards the cathode faster than in experiment Exp2.

For experiments Exp3 to Exp6, 50% iron slag-50% AC RFM was placed next to the cathode with the anolyte circulated to the cathode to control alkaline front transport in the soil. Experiment Exp4 was conducted for 2 weeks, and experiments Exp5 and Exp56 for 3 weeks. In experiments Exp4 and Exp5, the soil pH increased gradually from pH 3 in section S1 to about pH 3.7 in section S5 (**Figure 3a**). Compared to the latter experiments, the soil pH in experiment Exp6 remained constant at about pH 3 in sections S1 to S5 due to the rapid advancement of the acid front in the soil. The soil pH of section S6 increased and reached close to the soil pH (pH 4.24) in experiments Exp4 and Exp5 and pH 4 in experiment Exp6. The RFM pH was alkaline in all experiments but was slightly higher in experiment Exp2 (pH 11.4) with 100% iron slag RFM due to its higher initial pH (**Table 2**). In all experiments, lowering the soil pH to less than the initial soil pH will impart a positive charge onto the soil surface, decreasing the adsorption of metal ions.

Figure 3b shows the electric conductivity (EC) of the EK experiments. In experiments Exp1 to Exp3, the soil EC in sections S1 to S3 was more significant than the initial soil EC due to the high ionic strength of pore fluid caused by metal ions solubilization by the acid front. However, the soil EC decreased gradually in sections S4 to S6 due to the precipitation of metal ions or ions moving toward the cathode region in these experiments. In contrast, the soil EC in experiments Exp4 and Exp5 was greater than the initial soil EC in sections S1 to S4 due to the high ionic strength of pore fluid, then decreased to lower than the initial soil EC in sections S5 and S6 as a result of metal ions precipitation and transport toward the cathode. In experiment Exp6, the soil EC remained less than the initial soil EC because of ions migration towards the cathode and precipitation in the RFM, as discussed in section 3.4. Finally, the RFM EC in experiments Exp2 to Exp6 was greater than the initial soil EC because of the higher EC of initial iron slag and iron slag-AC than the initial soil EC (**Table 2**).

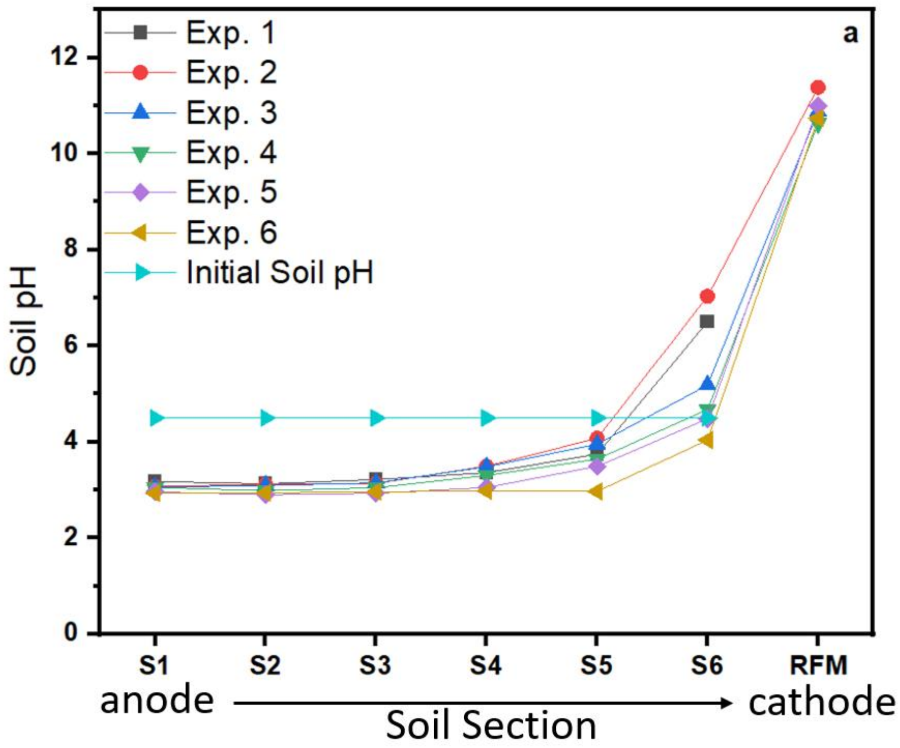

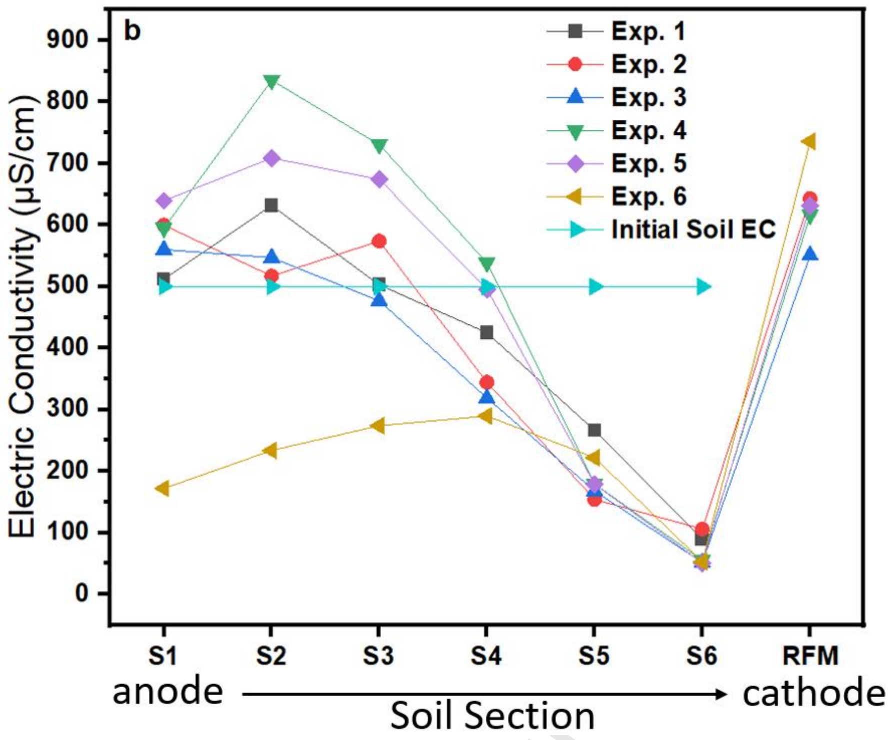

Figure 3: Soil pH and electric conductivity (EC) at the end of the EK experiments (a) soil pH and (b) electric conductivity.

3.3. Removal Rate

Six EK experiments were carried out to remove a single metal ion and a mixture of heavy metals from a contaminated kaolinite soil (**Table 3**). Experiments Exp1 to Exp3 were conducted without the anolyte recycling, whereas experiments Exp4 to Exp6 with the anolyte recycling to the cathode compartment. Experiments Exp1 to Exp4 lasted for 2 weeks whilst Exp5 and Exp6 lasted for 3 weeks, and the latter tested to remove a mixture of heavy metals.

Heavy metal ions moved across the soil from the anode to accumulate in the soil sections near the cathode after being solubilized by the acid front developed from the electrolysis reaction at the cathode. In the experiment, Exp1, copper ions (Cu^{2+}) were solubilized by the low pH front and transported across the soil from section S1 to S6. Generally, when pH drops below the point of zero charges (pzc), the soil surface charge will be positive, reducing the adsorption of metal ions. Therefore, the copper concentration was removed almost entirely from section S1, increased progressively in sections S2 to S5, and increased dramatically to 3486 mg/L in section S6 (**Figure 3a**). However, the amount of copper removed from the soil was about 3.11% (**Figure 4g**). Applying iron slag RFM near the cathode in experiment Exp2 increased copper removal from the soil section S1 to S5 (**Figure 4b**), and most of the copper was precipitated in section S6 as the soil pH became alkaline (**Figure 3a**). The copper concentration was 44 mg/L in section S1 and increased to 4242 mg/L in section S6. Only 81 mg/L copper concentration was found in the iron slag RFM, and 23.36% copper removal was achieved in the experiment Exp2 (**Figure 4g**). Iron oxide, the primary component of iron slag, has a strong adsorption capacity to heavy metals, e.g., copper, nickel, and zinc (Yeongkyoo, 2018). The mechanisms of retaining heavy metals by iron oxide include surface complexation, precipitation, and electrostatic interactions (Hu et al., 2018). Despite copper removal in experiment Exp2 being 7 times greater than in experiment Exp1, the removal rate is still low, with only 21.6% of the copper captured by the RFM (**Table 4**). The alkaline conditions in section S6 favoured copper precipitation. Using iron slag-AC (50%-50%) RFM in the experiment Exp3 improved the copper removal from most soil sections, and 62.5% of the copper was accumulated in the RFM (**Table 4**). The copper concentration increased from 71 mg/L in the soil section S1 to 613 mg/L in section S6, reaching 4400 mg/L in the RFM (**Figure 4c**). The prevalent acid condition in most soil sections in experiment Exp3 enhanced the copper removal greater than in experiment Exp2. Also, incorporating AC in the RFM hampered the rapid advancement of the alkaline front.

To further improve the removal of heavy metal ions from the soil, the anolyte was recycled to the cathode compartment to neutralize the alkaline pH in experiments Exp4 to Exp6. As shown in **Figure 4d**, copper was removed from soil sections S1 to S6 and accumulated in the RFM of experiment Exp4. The concentration of copper in section S1 was 33 mg/L and increased to 261 mg/L in section S6, whilst it reached 6549 mg/L in the RFM. Almost 81.8% of the copper was accumulated in the RFM (**Table 4**), and the total copper removal in experiment Exp6 was 89.21% (**Figure 4g**). The greater copper removal in experiment Exp4 compared to experiment Exp3 was attributed to the anolyte recirculation to the cathode compartment, neutralizing alkaline pH. As a result, the acid front swept across the soil, solubilized, and carried the copper ions towards the RFM. Experiment Exp5 evaluated the impact of the EK duration on the copper ion removal by extending the EK process to 21 days (**Table 3**). **Figure 4e** shows that copper concentration in the soil sections S1 to S5 remained less than 50 mg/L and moderately increased to 198 mg/L in section S6. Copper removal in the soil sections S1 to S5 was about 99% and decreased slightly to 96% in section S6. Anolyte recirculation to the cathode compartment neutralized the alkaline front and promoted the acid front advancement in the soil, carrying the copper ions to the RFM section in experiment Exp5. The total copper removal at the end of the 3 weeks EK process was 93.45% (**Table 4**), about 5% greater than in the experiment Exp4. Experiment Exp6 evaluated the efficiency of the EK process coupled with iron slag-AC RFM, and anolyte was recycled to the cathode compartment. In addition to copper, nickel, and zinc were spiked into the kaolinite soil at 1 g/L to simulate the EK process treating a mixture of contaminants. The acid front swept across the soil in experiment Exp6, dissolved, and transported heavy metals to the RFM near the cathode region (**Figure 4f**). Copper, nickel, and zinc concentrations decreased gradually from the soil section S1 to S6 and accumulated in the RFM near the cathode. Furthermore, 71.7% of the copper, 83.9% of nickel, and 89.2% of zinc were captured by the RFM (**Table 4**). Copper, nickel, and zinc concentrations in the RFM are 5133 mg/L, 7302 mg/L, and 8191 mg/L, respectively. The corresponding removal of these heavy metals at the end of the EK process is 81.1% for copper, 89.09% for nickel, and 92.31% for zinc. The higher removal of nickel and zinc than copper is attributed to the pH of metal hydroxide precipitation, pH 6.9 for copper, pH 8.5 for zinc, and 8.8 for nickel (Kabdaşlı et al., 2012). Therefore, nickel and zinc removal was greater than copper at the end of experiment Exp6.

Copper removal increased from 3.11% (Exp1) to 23.36% (Exp2) when using iron slag RFM. Further increase in copper removal was achieved by mixing iron slag with AC in Exp3 due to the affinity of AC to alkaline pH. Anolyte recirculation to the cathode compartment in experiment Exp4 further improved copper removal in experiment Exp4 due to alkaline pH neutralization. Copper removal was 93.45 in experiment Exp5 when the EK processing was extended to 3 weeks. The EK efficiency was slightly affected in experiment Exp6 with a mixture of heavy metals. The total metals removal was between 81.1% and 92.31%, depending on their solubility. In such a case, the duration of the EK process must be extended to achieve the desired removal rate.

Placing the RFM near the cathode, where inorganic pollutants are expected to accumulate in the EK process, aims to adsorb heavy metals and facilitate their extraction at the end of the EK experiment. In experiment Exp1, the alkaline front swept across the soil section S6, where most of the copper precipitated as metal hydroxide. Incorporating iron slag RFM in experiment exp2 slightly improved copper removal from 3.11% in Exp2 to 23.36% in Exp3. Although iron slag improved copper adsorption to some extent, it was ineffective in preventing the movement of the alkaline front in experiment Exp2, resulting in most of the copper precipitating as metal hydroxide in section S6. Therefore, AC was added to the RFM due to its affinity to the hydroxyl ions, preventing alkaline front transport toward the anode. Copper removal increased to 70.14% in Exp3 and further increased to 89.21% in Exp4 when the anolyte was recirculated to the cathode zone.

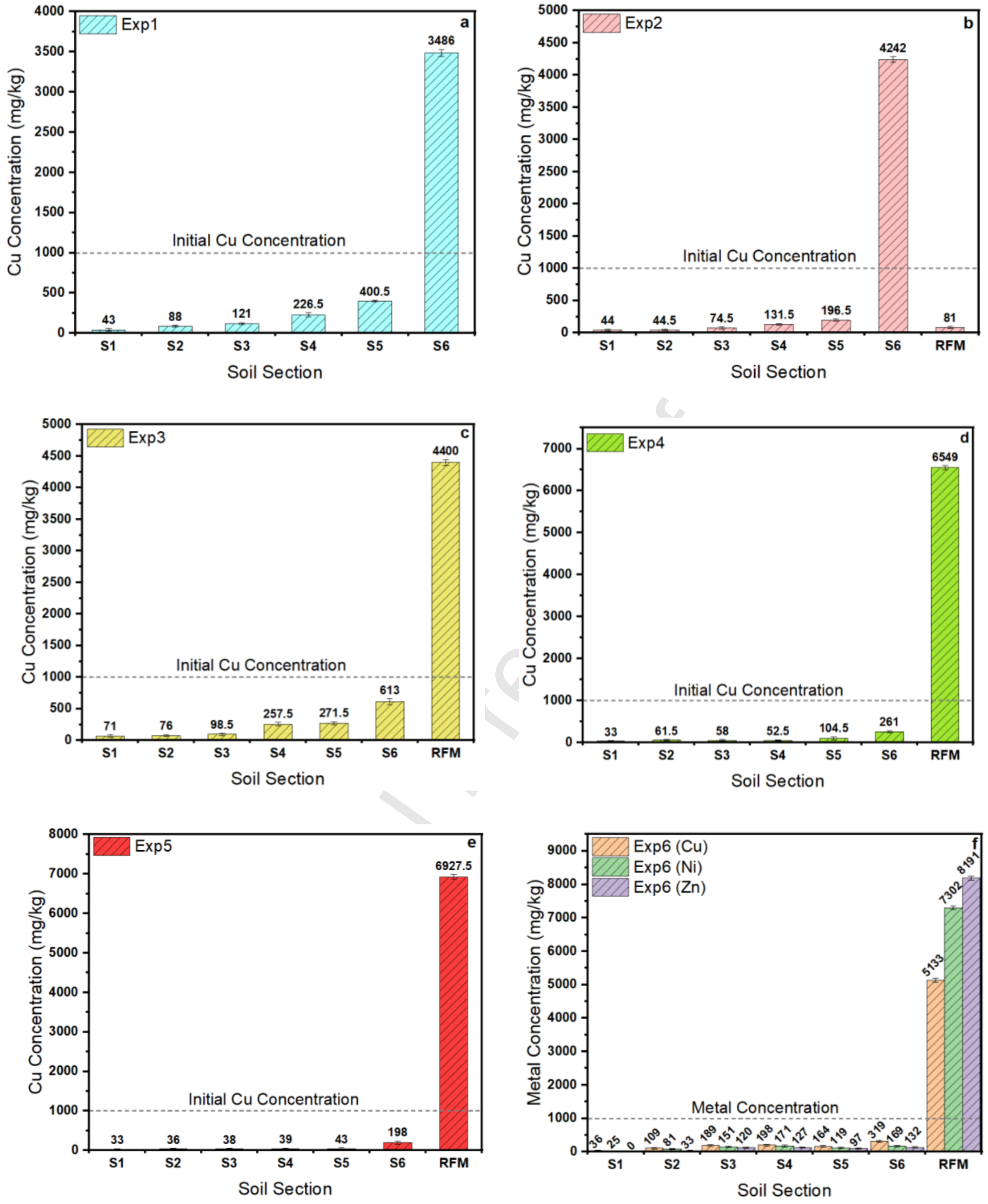
a
Exp1
Cu Concentration (mg/kg)
4000
3500
3000
2500
2000
1500
1000
500
0
Initial Cu Concentration
43
88
121
226.5
400.5
3486
S1
S2
S3
S4
S5
S6
Soil Section
b
Exp2
Cu Concentration (mg/kg)
5000
4500
4000
3500
3000
2500
2000
1500
1000
500
0
Initial Cu Concentration
44
44.5
74.5
131.5
196.5
4242
81
S1
S2
S3
S4
S5
S6
RFM
Soil Section
c
Exp3
Cu Concentration (mg/kg)
5000
4500
4000
3500
3000
2500
2000
1500
1000
500
0
Initial Cu Concentration
71
76
98.5
257.5
271.5
613
4400
S1
S2
S3
S4
S5
S6
RFM
Soil Section
d
Exp4
Cu Concentration (mg/kg)
7000
6000
5000
4000
3000
2000
1000
0
Initial Cu Concentration
33
61.5
58
52.5
104.5
261
6549
S1
S2
S3
S4
S5
S6
RFM
Soil Section
e
Exp5
Cu Concentration (mg/kg)
8000
7000
6000
5000
4000
3000
2000
1000
0
Initial Cu Concentration
33
36
38
39
43
198
6927.5
S1
S2
S3
S4
S5
S6
RFM
Soil Section
f
Exp6 (Cu)
Exp6 (Ni)
Exp6 (Zn)
Metal Concentration (mg/kg)
9000
8000
7000
6000
5000
4000
3000
2000
1000
0
Metal Concentration
36
25
0
109
81
33
189
151
120
198
171
127
164
119
97
319
169
132
5133
7302
8191
S1
S2
S3
S4
S5
S6
RFM
Soil Section

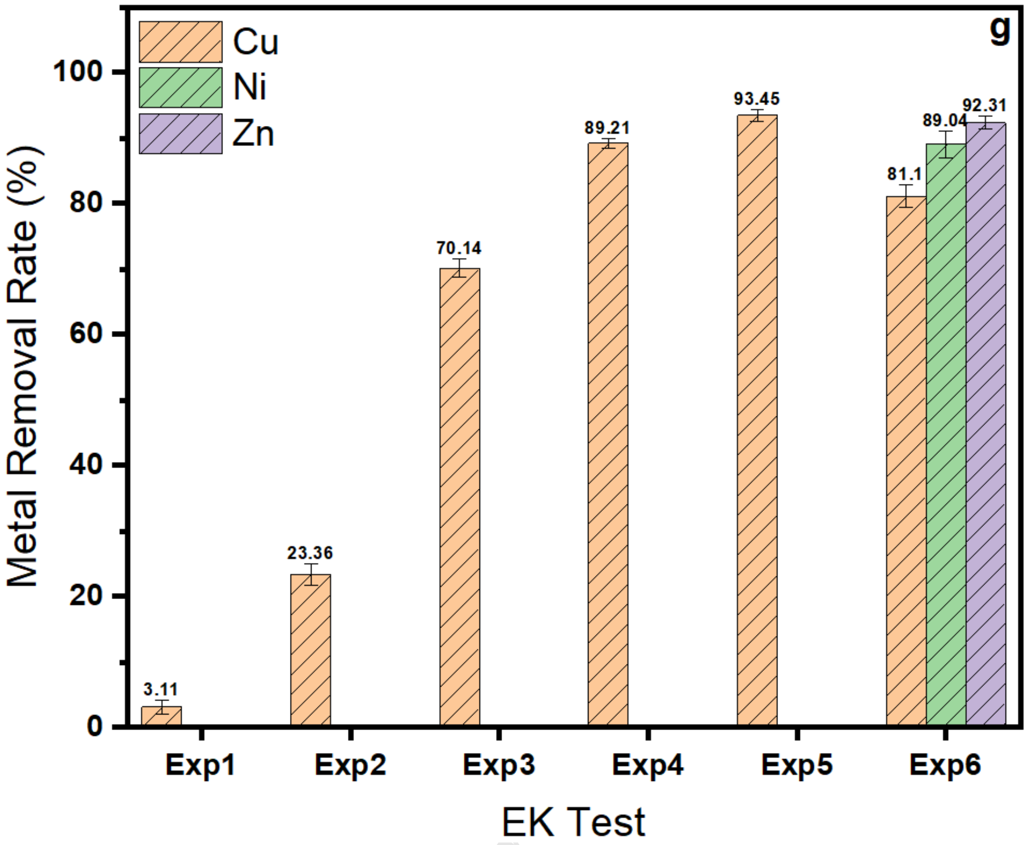

Figure 4: Cu in all experiments and Ni and Zn removal in experiment 6 at the end of the EK process

Table 4. EK experimental conditions for copper removal and its mass balances. The concentration of metal ions is 1 g/kg, and tests were conducted at 22 °C

Exp No	Metal ions	Residual metal ions in Soil (g)	Metal mass in RFM (g)	Mass Balance (%)	Removal (%)
Exp1	Cu	0.971	NA	102.97	3.11±0.23
Exp2	Cu	0.766	0.216	101.72	23.36±0.31
Exp3	Cu	0.297	0.625	103.27	70.14±0.28
Exp4	Cu	0.106	0.818	96.04	89.21±0.14
Exp5	Cu	0.065	0.844	97.88	93.45±0.19
Exp6	Cu	0.189	0.717	106.97	81.10±0.34
	Ni	0.109	0.839	102.98	89.04±0.39

Zn	0.076	0.892	103.22	92.31±0.20

3.4. Characteristics of RFM

Steel slag, a solid waste, possesses a high specific surface area and considerable porosity. These characteristics make them a promising candidate as an inexpensive adsorbent for eliminating pollutants from soil. The effectiveness of steel slag in removing contaminants depends on its unique characteristics and chemical composition. Activated carbon has traditionally been an adsorbent for removing heavy metals from polluted soil and water (Ahmed et al., 2015; Ghobadi et al., 2020). In our study, we utilized a mixture of activated carbon and iron slag, known as the RFM (Remediation Filter Material), in the electrokinetic (EK) process to adsorb copper, nickel, and zinc. **Figure 5a** showcases the X-ray diffraction (XRD) outcome of the constituents of the iron slag produced in the steel-making process. The findings underscore the prevalence of iron oxide as the predominant element within the iron slag composition. It is noteworthy that iron oxide possesses a notable adsorption capability, rendering it effective in the removal of contaminants (Díaz-Piloneta et al., 2022). While the precise nature of the interaction between iron oxide and Cu, Ni, and Zn remains a topic of ongoing investigation, it is established that iron oxide has the capacity for adsorption or surface attachment interactions with these elements in the surrounding environment. This propensity is attributed to the inherent attributes of iron oxide, including its diminutive particle dimensions and pronounced porosity, which collectively bestow upon it a significant surface area, thereby positioning it as an excellent adsorbent. The central process governing the adsorption of Cu, Ni, and Zn onto iron oxide revolves around electrostatic interactions among the molecules of these metals. This interaction is succeeded by forming inner-sphere Fe-carboxylate complexes through ligand exchange (Jain et al., 2018). The adsorption process involving Cu, Ni, and Zn onto iron oxide particles carries significant implications. Firstly, it diminishes the mobility of these elements within the environment, thereby mitigating the potential for groundwater contamination or seepage into the neighbouring regions. Moreover, this adsorption phenomenon can influence the behaviour and attributes of the iron oxide particles themselves. This influence extends to aspects encompassing stability and reactivity.

The functional properties of iron slag and iron slag/AC can be effectively assessed using FTIR spectra, which provide valuable information (Alhashimi and Aktas, 2017; Ghobadi et al., 2020). **Figure 5b** presents the FT-IR spectra of the new RFM, used RFM with iron slag, and used RFM with iron slag/AC. The FTIR spectra of both iron slag and iron slag/AC, both before and after the EK treatment, demonstrated similar characteristics. In contrast, the bands were more pronounced in the iron slag/AC before and after the EK treatment. This finding demonstrates the great promise of EK-iron slag/AC in eliminating copper, nickel, and zinc. After the EK treatment, the FTIR spectra of iron slag and iron slag/AC (refer to **Figure 5b**) exhibited peaks in the 3750, 2340, 1750, and 1550 cm^{-1} regions, indicating OH stretching. The band at 3750 cm^{-1} has diminished in Exp5 for Iron slag/AC; however, it has similar stretching in all the other experiments. The band at 2340 cm^{-1} has slightly increased in intensity after soil treatment with iron slag only in Exp2 due to the additional OH groups introduced by the iron slag, leading to a change in intensity. In all the experiments, this band has no visible change when the soil is treated with iron slag/AC. The FTIR band at 1750 cm^{-1} is diminished in Exp3 and Exp5 for iron slag/AC treatment, probably as a result of the adsorption of carbonyl groups (1750 cm^{-1}) by activated carbon (Stavropoulos et al., 2008).

SEM analysis combined with EDS (**Figure 5**) provided definitive evidence of the existence of copper, nickel, and zinc on the surfaces of RFMs following the electrokinetic (EK) treatment. SEM images showing surface morphologies and EDS graphs for the RFMs are presented in Figures 5c, 5d, 5e, and 5f. There is no presence of any contaminants on the surface of the RFMs. After treatment, contaminants observation was particularly evident in the iron slag and iron slag/AC specimens. The copper content in iron slag was lower than that in iron slag/AC RFM. According to the EDS results, the copper content was 1.19% in iron slag/AC and merely 0.34% in iron slag, indicating that copper removal through the EK treatment using iron slag/AC RFM was more effective than iron slag RFM. Significant changes in the surface morphology of RMSs are also observed after treatment with both methods, as evident from the SEM images in Figures 5g, 5i, and 5k. The presence of copper, nickel and zinc is also apparent in these images, as indicated by the respective colours.

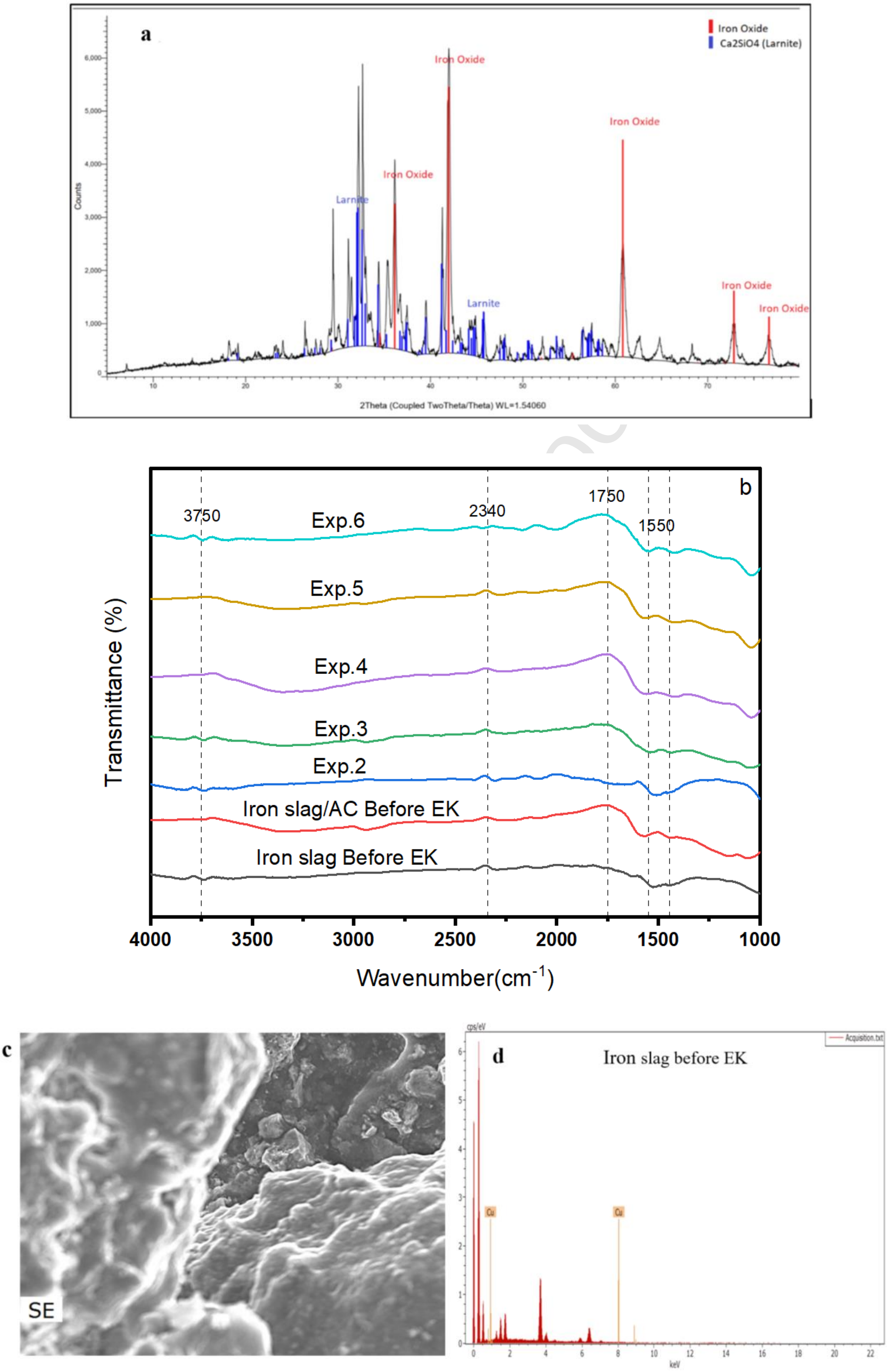
a
Iron Oxide
Ca2SiO4 (Larnite)
Iron Oxide
Iron Oxide
Larnite
Iron Oxide
Larnite
Iron Oxide
Iron Oxide
Counts
6,000
5,000
4,000
3,000
2,000
1,000
0
10
20
30
40
50
60
70
2Theta (Coupled TwoTheta/Theta) WL=1.54060
b
3750
2340
1750
1550
Exp.6
Exp.5
Exp.4
Exp.3
Exp.2
Iron slag/AC Before EK
Iron slag Before EK
Transmittance (%)
4000
3500
3000
2500
2000
1500
1000
Wavenumber(cm-1)
c
SE
d
Iron slag before EK
cps/eV
Acquisition.txt
Cu
Cu
6
5
4
3
2
1
0
0
2
4
6
8
10
12
14
16
18
20
22
keV

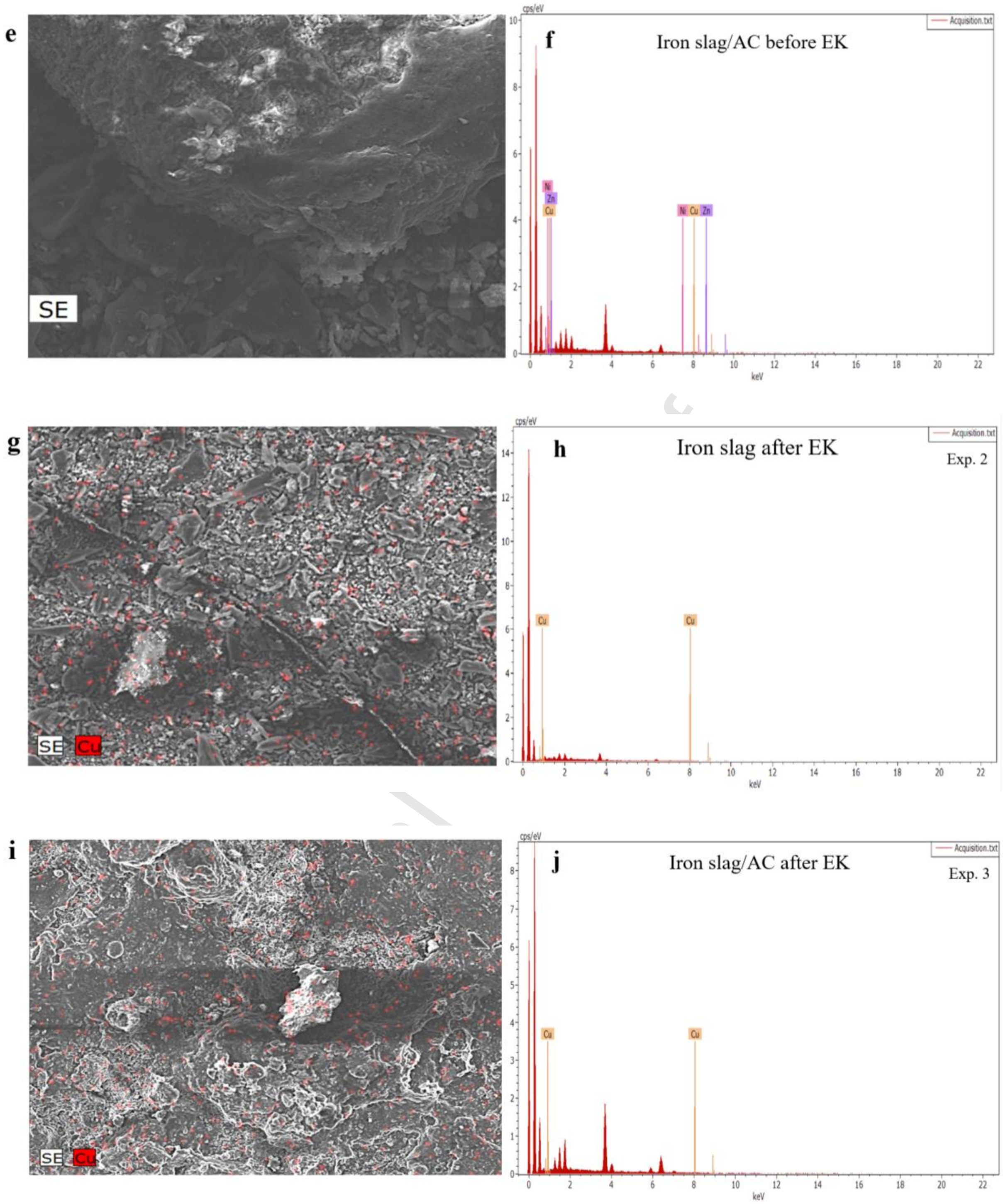
e
SE
f
Iron slag/AC before EK
cps/eV
Acquisition.txt
Ni
Zn
Cu
Ni
Cu
Zn
keV
0
2
4
6
8
10
12
14
16
18
20
22
g
SE
Cu
h
Iron slag after EK
Exp. 2
cps/eV
Acquisition.txt
Cu
Cu
keV
i
SE
Cu
j
Iron slag/AC after EK
Exp. 3
cps/eV
Acquisition.txt
Cu
Cu
keV

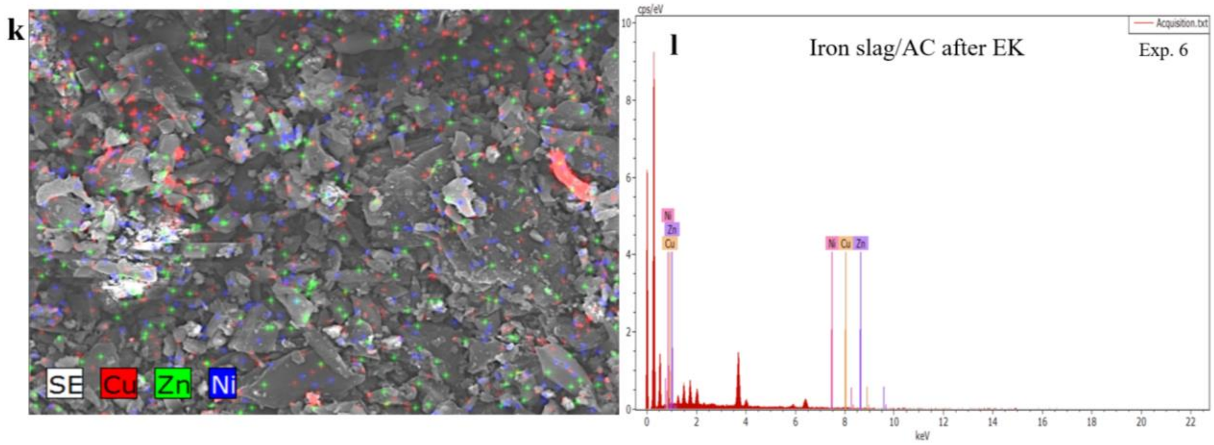

Figure 5: Iron slag XRD spectrum of (a), FTIR spectra of (b) iron slag before and after EK treatment (Exp2); iron slag/AC before and after EK treatment (Exp 3, 4, 5, 6), and SEM images of (c, d) iron slag, (e, f) iron slag/activated carbon before EK treatment; SEM and EDS of (g, h) iron slag, (i, j & k, l) iron slag/activated carbon after EK treatment.

3.5. RFM adsorption/desorption

The outcomes of dynamic adsorption trials utilizing iron slag/AC are portrayed in **Figures 6a and 6b**. The adsorption dynamics of heavy metals were exhaustively explored, revealing that iron slag achieves its highest adsorption capacity, amounting to 30.79 mg/g within 90 minutes for copper sulfate. In the case of the mixed solution, the values were 29.16 mg/g for copper sulfate, 13.11 mg/g for nickel chloride, and 11.45 mg/g for zinc sulfate. Initially, the extraction of heavy metals transpires rapidly, signifying a notable adsorption velocity. Nonetheless, as the system nears equilibrium, the adsorption process gradually synchronizes with the desorption rate. The extent of heavy metal assimilation and the pace of adsorption is influenced by diverse factors, including the duration of contact and the specific attributes of the iron slag/AC (Kulal and Badalamoole, 2020; Zhuang et al., 2016).

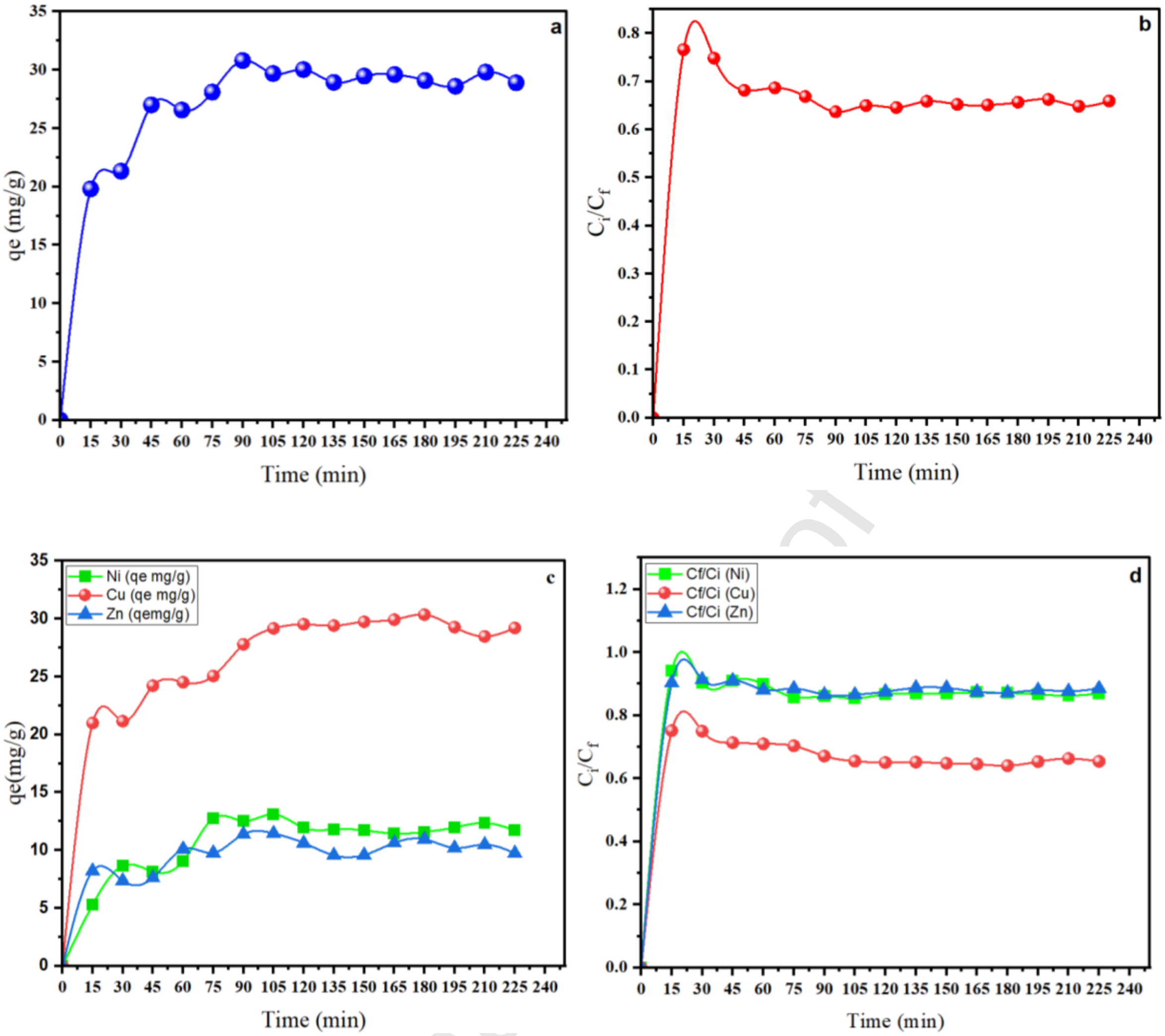
a
qe (mg/g)
0
5
10
15
20
25
30
35
Time (min)
0 15 30 45 60 75 90 105 120 135 150 165 180 195 210 225 240
b
C_i/C_f
0.0
0.1
0.2
0.3
0.4
0.5
0.6
0.7
0.8
Time (min)
0 15 30 45 60 75 90 105 120 135 150 165 180 195 210 225 240
c
Ni (qe mg/g)
Cu (qe mg/g)
Zn (qemg/g)
qe(mg/g)
0
5
10
15
20
25
30
35
Time (min)
0 15 30 45 60 75 90 105 120 135 150 165 180 195 210 225 240
d
Cf/Ci (Ni)
Cf/Ci (Cu)
Cf/Ci (Zn)
C_i/C_f
0.0
0.2
0.4
0.6
0.8
1.0
1.2
Time (min)
0 15 30 45 60 75 90 105 120 135 150 165 180 195 210 225 240

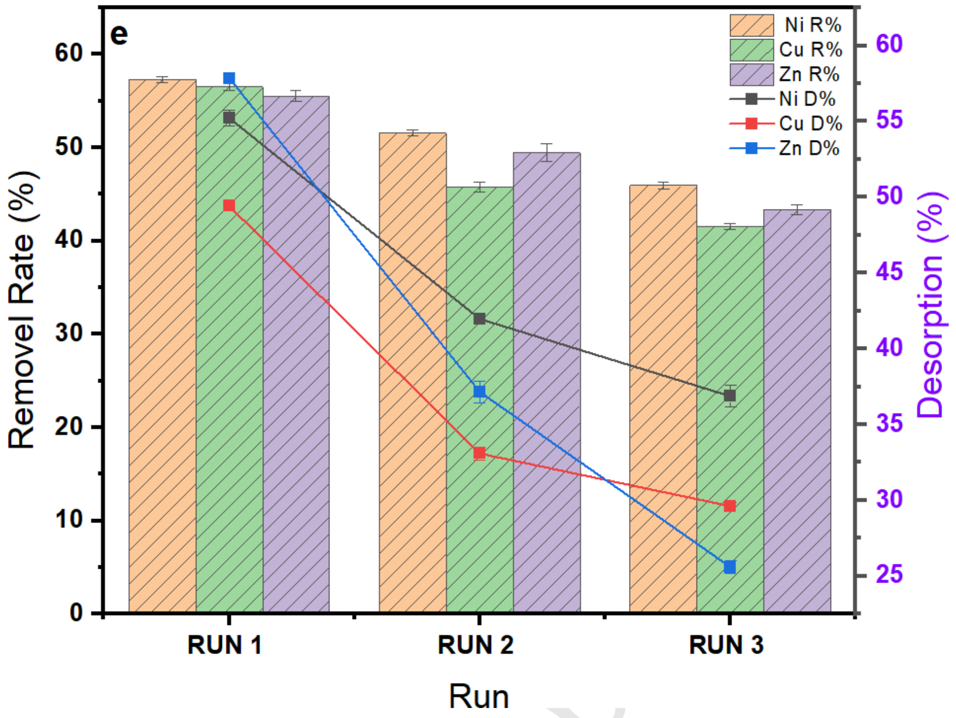

Figure 6: copper and mixed solution adsorption experiments, a) impact of iron slag/AC adsorption of $CuSO_4$ with time, b) The impact of contact time on the adsorption of metal ion (Cu), c) impact of iron slag/AC adsorption of mixed solution (Cu, Ni, Zn) with time, d) The effect of contact time on the adsorption of metal ion (Cu, Ni, Zn), e) Adsorption and desorption of Cu, Ni, and Zn across three successive cycles.

The dynamic adsorption tests using iron slag/AC revealed outcomes in **Figures 6c and 6d**. Initially, metal ions were quickly removed, indicating strong adsorption. However, as the system approached equilibrium, this removal rate slowed due to the increasing occupation of adsorption sites. The interaction between adsorbate molecules at these sites and those in the bulk phase caused a deceleration. The adsorbate extraction rate from the solution depended on their transition within the adsorbent material, from surface to interior. Equilibrium, where adsorption and desorption rates are balanced, was reached within 90 minutes for the studied metal ions (Rahchamani et al., 2011; Zhuang et al., 2016). Magnetite nanoparticles are electron contributors due to e^{2+} ions (Castro et al., 2018). The key approaches to extracting ions from water encompass electrostatic adsorption, the interaction of heavy metal ions with metal oxide surfaces, the exchange of metal ions in the solution with hydrogen derived from hydroxyl groups on the adsorbent's surface, and the creation of complexes. Adsorbents containing various chemical groups like carboxyl, hydroxyl, ester, aldehyde, and ketone can connect with metal ions. The strength of this connection depends on factors such as site count, accessibility, chemical structure, and binding nature (Jain et al., 2018).

Three adsorption-desorption cycles were executed with feed concentrations of 2.52 g/L, 2.21 g/L, and 2.51 g/L, each cycle lasting 24 hours to assess the sequential elimination of Cu, Ni, and Zn ions. Across the three cycles, the percentage of copper removal totalled 56.54%, 45.79%, and 41.96% of the initial Cu content. For nickel ions, the corresponding values were 57.3%, 51.54%, and 45.94%; for zinc, they were 55.54%, 49.46%, and 43.37%. Furthermore, the desorption concentrations after the three cycles were 49.42%, 33.09%, and 29.61% for copper, 55.22%, 41.96%, and 36.86% for nickel, and 57.86%, 37.15%, and 25.59% for zinc, as depicted in **Figure 6e**. The desorption process of iron slag/AC involves releasing previously held molecules or ions, occurring through mechanisms like diffusion, exchange reactions, solvent effects, and external triggers. Distribution follows concentration gradients, moving adsorbed species from high to low concentrations. Exchange reactions replace less-affine species with those having higher affinity. Solvents alter interactions between iron slag/AC and adsorbed species. External factors, such as variations in temperature, shifts in pH levels, structural adjustments, and the liberation of adsorbed species, can all lead to changes. In an acidic environment, protons compete with binding sites, weakening interactions and releasing adsorbed metal ions, underscoring the role of solution conditions in desorption.

3.6. Specific Energy Consumption

The magnitude of the operating current plays a crucial role in the electrokinetic process, exerting a profound influence on both the power consumption and reaction kinetics involved (Ghobadi et al., 2021b). Instead of increasing the electric current, the experimental time was extended to 21 days to enhance heavy metals removal in experiments Exp5 and Exp6. Elevating electric current enhances heavy metals migration but could lead to electrolyte depletion, soil heating, and surface damage. Alternatively, extending processing time allows for gradual metal dissolution without such risks. Therefore, in the later EK tests Exp5 and Exp6, the experimental time was extended to 21 days to avoid any consequences due to the increased electric current. **Figure 7** illustrates the variations in the removal rate of total heavy metals (specifically Cu, Ni, and Zn) concerning the dry soil mass, along with the corresponding specific energy consumption during the whole experiment of the EK-RFM process. These changes are depicted under various experimental conditions and enhancement factors. The study examined the effects of processing time and current intensity to assess the removal rate and energy consumption. These factors were carefully investigated, and their impact is reflected in **Figure 7**. Significant removal rates of nickel (Ni), copper (Cu), and zinc (Zn) were observed in all tests that were conducted. The analysis of power consumption indicated a significant rise in specific energy consumption (SEC) within the EK-RFM system when altering the duration of treatment. The specific energy consumption (SEC) is at the high end, elevating from 0.055 kWh/kg to 0.14 kWh/kg for the treated soil. The comparison between Experiment 3 and Experiment 4 revealed that implementing anolyte recycling increased the overall copper removal rate. Significantly, this observed enhancement in the removal rate was concomitant with a reduction in energy consumption, declining from 0.12 kWh/kg to 0.10 kWh/kg while maintaining a constant current of 20 mA. Experiment 5 exhibited a significant augmentation in energy consumption, reaching a value of 0.14 kWh/kg during the electrokinetic (EK) remediation procedure as the duration of processing was prolonged. Nevertheless, notwithstanding the escalated energy consumption, the overall removal rate remained consistently high, fluctuating between 89.21% and 93.45%.

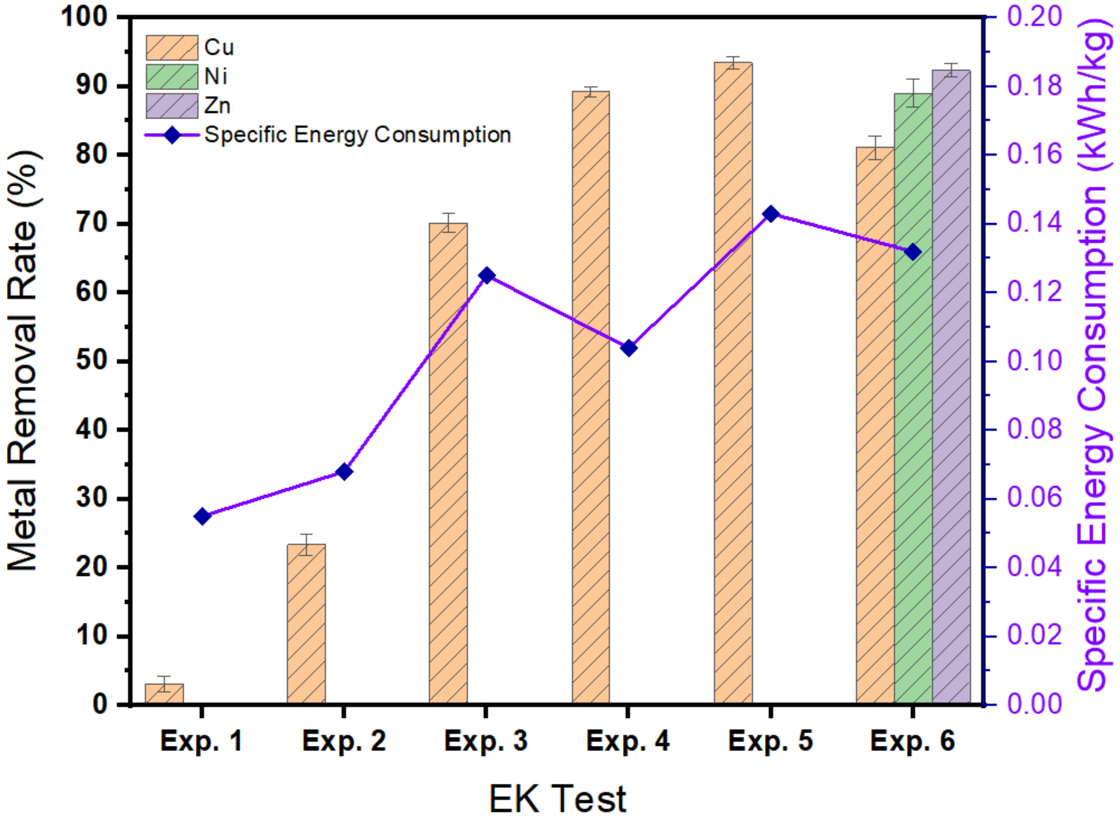

Figure 7: Total Cu, Ni, and Zn removal and specific energy consumption during EK

The findings from the EK tests indicate a noteworthy decrease in power consumption due to the implementation of anolyte recycling. Typically, the incorporation of anolyte recycling within the electrokinetic (EK) process results in a reduction in specific power consumption. The findings from Experiment 6 underscored the importance of the electric current in the electrokinetic process. In the context of handling copper, nickel, and zinc mixtures, the efficacy of completely removing copper declined from 93.45% to 81.10% due to the necessity to allocate the electric current across the three constituent elements. Previous studies by Ghobadi et al. (2021 and 2020) suggest that increasing the electric current would enhance the copper, nickel, and zinc treatment process.

Although EK tests with RFMs consumed higher energy, they achieved better heavy metals removal than the EK without RFMs. The higher electric conductivity of RFMs, 0.551 ms/cm to 0.643 ms/cm, compared to the kaolinite soil, 0.39 ms/cm, affected the power consumption in the EK process. Undoubtedly, the EK tests without RFMs required less energy to perform than those with the RFMs, but that was at the expense of heavy metal removal. RFM experiments achieved 23.36% to 93.45% copper removal compared to 3.11% in the EK without RFM. The higher energy consumption in experiments Exp5 and Exp6 also stems from extending the experimental time to 3 weeks.

4. Conclusion

The EK process was coupled with iron slag or iron slag-AC RFM for a single or a mixture of heavy metals removal from kaolinite soil. Heavy metals removal increased from 3.11% in the EK process to 23.26% in the iron slag-EK process. The alkaline pH of the iron slag promoted metal ions adsorption and precipitation. More significant copper removal was achieved in the EK process coupled with iron slag-AC RFM due to hydroxyl ions adsorption on the AC. Therefore, copper removal reached 70.14% in the EK process with iron slag-AC RFM. In conventional EK processes, enhancement agents are used to improve heavy metals removal, but that would be at the expense of the remediation cost. This study proposed anolyte recirculation to the cathode compartment to neutralize alkaline pH and enhance heavy metals removal. This method will reduce the operation cost, remediation efficiency, and risk of handling acid or alkaline chemicals. Copper removal increased from 70.14% in the RFM-EK process without anolyte recirculation to 89.21% in the RFM-EK with anolyte recirculation. More copper removal was achieved when the RFM-EK process was extended to 3 weeks, recording 93.45% copper removal. Besides, the RFM-EK with anolyte recirculation was evaluated for a mixture of heavy metals removal. Experimental results showed 81.1% copper removal, 89.04 nickel removal, and 92.31% zinc removal after a 3-week test. Heavy metals removal in the latter test corresponded to its solubility; hence, longer experimental time could be required for a greater removal. The RFM-EK with anolyte recirculation should be tested in a pilot plant in the future to demonstrate its field efficiency. Addressing the management of iron slag-AC RFM post-treatment is crucial, given its potential contamination with adsorbed heavy metals and pollutants. Safe disposal methods, such as recycling the slag for industrial applications or encapsulating it in inert materials, need exploration to prevent environmental hazards. Furthermore, future research should prioritize sustainable and eco-friendly strategies for managing waste from electrokinetic remediation processes, ensuring effective remediation while minimizing adverse environmental impacts.

Appendix 1.

Figure A1 displays the pH profile of the cathode and anode compartments for experiments Exp3 to Exp6. Apart from experiment Exp3, the anolyte was recirculated to the catholyte compartment in these experiments to suppress the advancement of the alkaline front in the soil, hence allowing the acid front to sweep across the soil. For experiments Exp4 and Exp5, the catholyte pH was pH 12.8 on day one, decreased over time and reached pH 9.5 after 14 days. Compared to experiment Exp3, the sharp reduction in the catholyte pH of experiments Exp4 and Exp5 is due to the anolyte recirculation to the cathode compartment, neutralizing the alkaline pH. The sharpest decline in the catholyte pH occurred in experiment Exp6, which treats a heavy metal mixture. The anolyte pH of experiments Exp3 to Exp6 was between pH 2.3 and 3.7 on day one and remained acidic for the rest of the experiments. The fluctuation of anolyte pH in experiment Exp6 was probably due to the changes in the ionic strength of the pore fluid due to the solubilization and precipitation of metal ions.

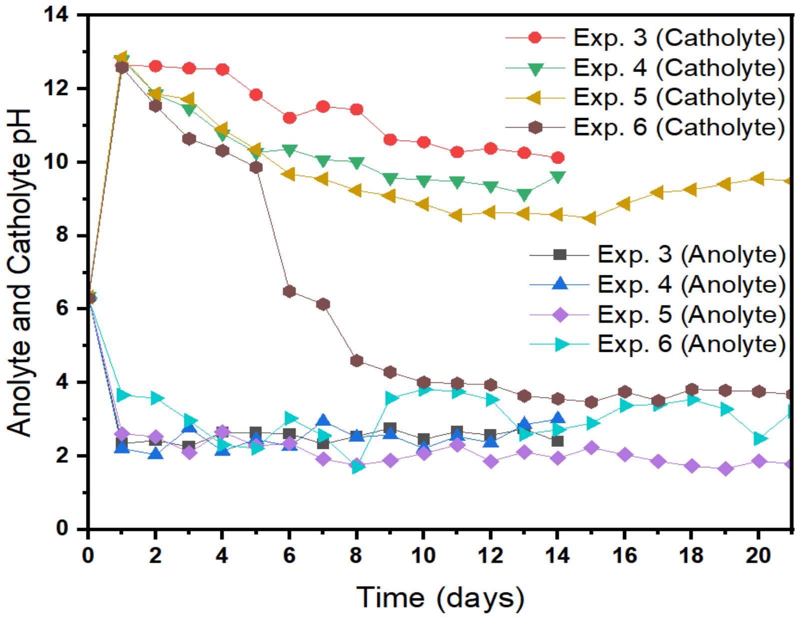

Figure A1: Exp3 no circulation operation times 14 days, Exp4 circulation operation times 14 days, and Exp5 & Exp6 circulation operation times 21 days.

Acknowledgments

The author would like to thank the Ministry of Government of Saudi Arabia for providing scholarship support to Faris M. Hamdi.

This research is made possible by a food security research award (MME03-1015-210003) from the Qatar National Research Fund (QNRF) in partnership with the Ministry of Municipality. The statements made herein are solely the responsibility of the authors.

References

Acar, Y.B., Alshawabkeh, A.N., 1993. Principles of electrokinetic remediation. Environ Sci Technol 27, 2638–2647. https://doi.org/10.1021/es00049a002

Agnew, K., Cundy, A.B., Hopkinson, L., Croudace, I.W., Warwick, P.E., Purdie, P., 2011. Electrokinetic remediation of plutonium-contaminated nuclear site wastes: Results from a pilot-scale on-site trial. J Hazard Mater 186, 1405–1414. https://doi.org/10.1016/J.JHAZMAT.2010.12.016

Ahmed, M.B., Zhou, J.L., Ngo, H.H., Guo, W., 2015. Adsorptive removal of antibiotics from water and wastewater: Progress and challenges. Science of The Total Environment 532, 112–126. https://doi.org/10.1016/J.SCITOTENV.2015.05.130

Alhashimi, H.A., Aktas, C.B., 2017. Life cycle environmental and economic performance of biochar compared with activated carbon: A meta-analysis. Resour Conserv Recycl 118, 13–26. https://doi.org/10.1016/J.RESCONREC.2016.11.016

Altaee, A., Smith, R., Mikhalovsky, S., 2008. The feasibility of decontamination of reduced saline sediments from copper using the electrokinetic process. J Environ Manage 88, 1611–1618. https://doi.org/10.1016/J.JENVMAN.2007.08.008

Bahemmat, M., Farahbakhsh, M., Kianirad, M., 2016. Humic substances-enhanced electroremediation of heavy metals contaminated soil. J Hazard Mater 312, 307–318. https://doi.org/10.1016/j.jhazmat.2016.03.038

Cang, L., Zhou, D.M., Wu, D.Y., Alshawabkeh, A.N., 2009a. Coupling electrokinetics with permeable reactive barriers of zerovalent iron for treating a chromium contaminated soil. Sep Sci Technol 44, 2188–2202. https://doi.org/10.1080/01496390902976699

Cang, L., Zhou, D.-M., Wu, D.-Y., Alshawabkeh, A.N., 2009b. Coupling Electrokinetics with Permeable Reactive Barriers of Zerovalent Iron for Treating a Chromium Contaminated Soil. Sep Sci Technol 44, 2188–2202. https://doi.org/10.1080/01496390902976699

Castro, L., Blázquez, M.L., González, F., Muñoz, J.A., Ballester, A., 2018. Heavy metal adsorption using biogenic iron compounds. Hydrometallurgy 179, 44–51. https://doi.org/10.1016/j.hydromet.2018.05.029

Díaz-Piloneta, M., Ortega-Fernández, F., Terrados-Cristos, M., Álvarez-Cabal, J.V., 2022. Application of Steel Slag for Degraded Land Remediation. Land (Basel) 11, 224. https://doi.org/10.3390/land11020224

Ganbat, N., Altaee, A., Zhou, J.L., Lockwood, T., Al-Juboori, R.A., Hamdi, F.M., Karbassiyazdi, E., Samal, A.K., Hawari, A., Khabbaz, H., 2022. Investigation of the effect of surfactant on the electrokinetic treatment of PFOA contaminated soil. Environ Technol Innov 28, 102938. https://doi.org/10.1016/J.ETI.2022.102938

Ghobadi, R., Altaee, A., Zhou, J.L., Karbassiyazdi, E., Ganbat, N., 2021a. Effective remediation of heavy metals in contaminated soil by electrokinetic technology incorporating reactive filter media. Science of The Total Environment 794, 148668. https://doi.org/10.1016/j.scitotenv.2021.148668

Ghobadi, R., Altaee, A., Zhou, J.L., McLean, P., Ganbat, N., Li, D., 2021b. Enhanced copper removal from contaminated kaolinite soil by electrokinetic process using compost reactive filter media. J Hazard Mater 402, 123891. https://doi.org/10.1016/J.JHAZMAT.2020.123891

Ghobadi, R., Altaee, A., Zhou, J.L., McLean, P., Yadav, S., 2020. Copper removal from contaminated soil through electrokinetic process with reactive filter media. Chemosphere 252, 126607. https://doi.org/10.1016/J.CHEMOSPHERE.2020.126607

Gholizadeh, M., Hu, X., 2021. Removal of heavy metals from soil with biochar composite: A critical review of the mechanism. J Environ Chem Eng 9, 105830. https://doi.org/10.1016/J.JECE.2021.105830

Gong, Y., Zhao, D., Wang, Q., 2018. An overview of field-scale studies on remediation of soil contaminated with heavy metals and metalloids: Technical progress over the last decade. Water Res 147, 440–460. https://doi.org/10.1016/j.watres.2018.10.024

Groenenberg, J.E., Römkens, P.F.A.M., Zomeren, A. Van, Rodrigues, S.M., Comans, R.N.J., 2017. Evaluation of the Single Dilute (0.43 M) Nitric Acid Extraction to Determine Geochemically

Reactive Elements in Soil. Environ Sci Technol 51, 2246–2253. https://doi.org/10.1021/acs.est.6b05151

Hu, S., Lu, Y., Peng, L., Wang, P., Zhu, M., Dohnalkova, A.C., Chen, H., Lin, Z., Dang, Z., Shi, Z., 2018. Coupled Kinetics of Ferrihydrite Transformation and As(V) Sequestration under the Effect of Humic Acids: A Mechanistic and Quantitative Study. Environ Sci Technol acs.est.8b03492. https://doi.org/10.1021/acs.est.8b03492

Jain, M., Yadav, M., Kohout, T., Lahtinen, M., Garg, V.K., Sillanpää, M., 2018. Development of iron oxide/activated carbon nanoparticle composite for the removal of Cr(VI), Cu(II) and Cd(II) ions from aqueous solution. Water Resour Ind 20, 54–74. https://doi.org/10.1016/j.wri.2018.10.001

Kabdaşlı, I., Arslan-Alaton, I., Ölmez-Hancı, T., Tünay, O., 2012. Electrocoagulation applications for industrial wastewaters: a critical review. Environmental Technology Reviews 1, 2–45. https://doi.org/10.1080/21622515.2012.715390

Kulal, P., Badalamoole, V., 2020. Hybrid nanocomposite of kappa-carrageenan and magnetite as adsorbent material for water purification. Int J Biol Macromol 165, 542–553. https://doi.org/10.1016/j.ijbiomac.2020.09.202

Li, J., Ding, Y., Wang, K., Li, N., Qian, G., Xu, Y., Zhang, J., 2020. Comparison of humic and fulvic acid on remediation of arsenic contaminated soil by electrokinetic technology. Chemosphere 241, 125038. https://doi.org/10.1016/J.CHEMOSPHERE.2019.125038

Lim, M.W., Lau, E. Von, Poh, P.E., 2016. A comprehensive guide of remediation technologies for oil contaminated soil — Present works and future directions. Mar Pollut Bull 109, 14–45. https://doi.org/10.1016/J.MARPOLBUL.2016.04.023

Mao, X., Jiang, R., Xiao, W., Yu, J., 2015. Use of surfactants for the remediation of contaminated soils: A review. J Hazard Mater 285, 419–435. https://doi.org/10.1016/j.jhazmat.2014.12.009

Peppicelli, C., Cleall, P., Sapsford, D., Harbottle, M., 2018. Changes in metal speciation and mobility during electrokinetic treatment of industrial wastes: Implications for remediation and resource recovery. Science of The Total Environment 624, 1488–1503. https://doi.org/10.1016/J.SCITOTENV.2017.12.132

Rahchamani, J., Mousavi, H.Z., Behzad, M., 2011. Adsorption of methyl violet from aqueous solution by polyacrylamide as an adsorbent: Isotherm and kinetic studies. Desalination 267, 256–260. https://doi.org/10.1016/j.desal.2010.09.036

Ren, L., Lu, H., He, L., Zhang, Y., 2014. Enhanced electrokinetic technologies with oxidization–reduction for organically-contaminated soil remediation. Chemical Engineering Journal 247, 111–124. https://doi.org/10.1016/J.CEJ.2014.02.107

Song, B., Zeng, G., Gong, J., Liang, J., Xu, P., Liu, Z., Zhang, Y., Zhang, C., Cheng, M., Liu, Y., Ye, S., Yi, H., Ren, X., 2017. Evaluation methods for assessing effectiveness of in situ remediation of soil and sediment contaminated with organic pollutants and heavy metals. Environ Int 105, 43–55. https://doi.org/10.1016/J.ENVINT.2017.05.001

Stavropoulos, G.G., Samaras, P., Sakellaropoulos, G.P., 2008. Effect of activated carbons modification on porosity, surface structure and phenol adsorption. J Hazard Mater 151, 414–421. https://doi.org/10.1016/j.jhazmat.2007.06.005

Tian, Y., Boulangé-Lecomte, C., Benamar, A., Giusti-Petrucciani, N., Duflot, A., Olivier, S., Frederick, C., Forget-Leray, J., Portet-Koltalo, F., 2017. Application of a crustacean bioassay to evaluate a multi-contaminated (metal, PAH, PCB) harbor sediment before and after electrokinetic remediation using eco-friendly enhancing agents. Science of The Total Environment 607–608, 944–953. https://doi.org/10.1016/J.SCITOTENV.2017.07.094

Wen, D., Fu, R., Li, Q., 2021. Removal of inorganic contaminants in soil by electrokinetic remediation technologies: A review. J Hazard Mater 401, 123345. https://doi.org/10.1016/j.jhazmat.2020.123345

Xie, N., Chen, Z., Wang, H., You, C., 2021. Activated carbon coupled with citric acid in enhancing the remediation of Pb-Contaminated soil by electrokinetic method. J Clean Prod 308, 127433. https://doi.org/10.1016/j.jclepro.2021.127433

Xue, F., Yan, Y., Xia, M., Muhammad, F., Yu, L., Xu, F., Shiau, Y., Li, D., Jiao, B., 2017. Electrokinetic remediation of chromium-contaminated soil by a three-dimensional electrode coupled with a permeable reactive barrier. RSC Adv 7, 54797–54805. https://doi.org/10.1039/C7RA10913J

Yeongkyoo, K., 2018. Effects of different oxyanions in solution on the precipitation of jarosite at room temperature. J Hazard Mater 353, 118–126. https://doi.org/10.1016/j.jhazmat.2018.04.016

Yeung, A.T., 2011. Milestone developments, myths, and future directions of electrokinetic remediation. Sep Purif Technol 79, 124–132. https://doi.org/10.1016/J.SEPPUR.2011.01.022

Yu, X., Muhammad, F., Yan, Y., Yu, L., Li, H., Huang, X., Jiao, B., Lu, N., Li, D., 2019. Effect of chemical additives on electrokinetic remediation of Cr-contaminated soil coupled with a permeable reactive barrier. R Soc Open Sci 6, 182138. https://doi.org/10.1098/rsos.182138

Yuan, C., Chiang, T.S., 2007. The mechanisms of arsenic removal from soil by electrokinetic process coupled with iron permeable reaction barrier. Chemosphere 67, 1533–1542. https://doi.org/10.1016/J.CHEMOSPHERE.2006.12.008

Yuan, L., Li, H., Xu, X., Zhang, J., Wang, N., Yu, H., 2016a. Electrokinetic remediation of heavy metals contaminated kaolin by a CNT-covered polyethylene terephthalate yarn cathode. Electrochim Acta 213, 140–147. https://doi.org/10.1016/j.electacta.2016.07.081

Yuan, L., Xu, X., Li, H., Wang, N., Guo, N., Yu, H., 2016b. Development of novel assisting agents for the electrokinetic remediation of heavy metal-contaminated kaolin. Electrochim Acta 218, 140–148. https://doi.org/10.1016/J.ELECTACTA.2016.09.121

Zhao, S., Fan, L., Zhou, M., Zhu, X., Li, X., 2016. Remediation of Copper Contaminated Kaolin by Electrokinetics Coupled with Permeable Reactive Barrier. Procedia Environ Sci 31, 274–279. https://doi.org/10.1016/J.PROENV.2016.02.036

Zhuang, Y., Yu, F., Chen, J., Ma, J., 2016. Batch and column adsorption of methylene blue by graphene/alginate nanocomposite: Comparison of single-network and double-network hydrogels. J Environ Chem Eng 4, 147–156. https://doi.org/10.1016/j.jece.2015.11.014